

1 **Birth of a photosynthetic chassis: a MoClo toolkit enabling synthetic biology in the**  
2 **microalga *Chlamydomonas reinhardtii***

3 **Crozet Pierre<sup>1#</sup>, Navarro Francisco J<sup>2#</sup>, Willmund Felix<sup>3#</sup>, Mehrshahi Payam<sup>2#</sup>, Bakowski**  
4 **Kamil<sup>4</sup>, Lauersen Kyle J<sup>5</sup>, Pérez-Pérez Maria-Esther<sup>6</sup>, Auroy Pascaline<sup>7</sup>, Gorchs Rovira Aleix<sup>2</sup>,**  
5 **Sauret-Gueto Susana<sup>2</sup>, Niemeyer Justus<sup>3</sup>, Spaniol Benjamin<sup>3</sup>, Theis Jasmine<sup>3</sup>, Trösch**  
6 **Raphael<sup>3</sup>, Westrich Lisa-Desiree<sup>3</sup>, Vavitsas Konstantinos<sup>4</sup>, Baier Thomas<sup>5</sup>, Hübner**  
7 **Wolfgang<sup>8</sup>, de Carpentier Felix<sup>1</sup>, Cassarini Mathieu<sup>1</sup>, Danon Antoine<sup>1</sup>, Henri Julien<sup>1</sup>,**  
8 **Marchand Christophe H<sup>1</sup>, de Mia Marcello<sup>1</sup>, Sarkissian Kevin<sup>1</sup>, Baulcombe David C<sup>2</sup>, Peltier**  
9 **Gilles<sup>7</sup>, Crespo José-Luis<sup>6</sup>, Kruse Olaf<sup>5</sup>, Jensen Poul Erik<sup>4</sup>, Schroda Michael<sup>3\*</sup>, Smith Alison**  
10 **G<sup>2\*</sup> and Lemaire Stéphane D<sup>1\*</sup>**

11 <sup>1</sup>*Institut de Biologie Physico-Chimique, UMR 8226, CNRS, Sorbonne Université, Paris, France*

12 <sup>2</sup>*Department of Plant Sciences, University of Cambridge, Cambridge, CB2 3EA, UK*

13 <sup>3</sup>*Department of Biology, Technische Universität Kaiserslautern, Kaiserslautern, Germany*

14 <sup>4</sup>*Copenhagen Plant Science Centre, Dept. Plant and Environmental Sciences, University of*  
15 *Copenhagen, Copenhagen, Denmark*

16 <sup>5</sup>*Center for Biotechnology, Bielefeld University, Bielefeld, Germany*

17 <sup>6</sup>*Instituto de Bioquímica Vegetal y Fotosíntesis, CSIC-Universidad de Sevilla, Sevilla, Spain*

18 <sup>7</sup>*Aix Marseille Univ, CEA, CNRS, BIAM, Laboratoire de Bioénergétique et Biotechnologie des*  
19 *Bactéries et Microalgues, Cadarache, Saint Paul-Lez-Durance, France*<sup>8</sup>*Biomolecular*

20 *Photonics, Department of Physics, Bielefeld University, Bielefeld, Germany*

21 #these authors contributed equally to the work.

22 \*To whom correspondence should be addressed

23 \*S.D. Lemaire: Tel: +33 (0)628345239. Fax: +33 (0)158415025. [stephane.lemaire@ibpc.fr](mailto:stephane.lemaire@ibpc.fr)

24 \*A.G. Smith: Tel: +44 1223 333952. Fax: +44-1223-333953. [as25@cam.ac.uk](mailto:as25@cam.ac.uk)

25 \*M. Schroda: Tel: +49(0)631 205 2697. Fax: +49(0)631 205 2999. [schroda@bio.uni-kl.de](mailto:schroda@bio.uni-kl.de)

26

27 **Abstract**

28 Microalgae are regarded as promising organisms to develop innovative concepts based on  
29 their photosynthetic capacity that offers more sustainable production than heterotrophic  
30 hosts. However, to realize their potential as green cell factories, a major challenge is to make  
31 microalgae easier to engineer. A promising approach for rapid and predictable genetic  
32 manipulation is to use standardized synthetic biology tools and workflows. To this end we  
33 have developed a Modular Cloning toolkit for the green microalga *Chlamydomonas*  
34 *reinhardtii*. It is based on Golden Gate cloning with standard syntax, and comprises 119 openly  
35 distributed genetic parts, most of which have been functionally validated in several strains. It  
36 contains promoters, UTRs, terminators, tags, reporters, antibiotic resistance genes, and  
37 introns cloned in various positions to allow maximum modularity. The toolkit enables rapid  
38 building of engineered cells for both fundamental research and algal biotechnology. This work  
39 will make *Chlamydomonas* the next chassis for sustainable synthetic biology.

40

41 **Keywords:** Algal biotechnology, *Chlamydomonas reinhardtii*, modular cloning, synthetic  
42 biology.

43

44

45 There is an urgent need to decarbonize the world economy due to depletion of fossil fuel  
46 reserves coupled with accumulation of greenhouse gases produced by their combustion. One  
47 alternative to the use of fossil fuels is to use photosynthetic microorganisms, such as  
48 microalgae, as green cell factories to produce fuels and chemicals from atmospheric CO<sub>2</sub> in a  
49 sustainable process driven by sunlight<sup>1, 2</sup>. The fixed carbon can be redirected towards  
50 compounds that can be used in the fuel, food, cosmetic and pharmaceutical industries, such  
51 as proteins, alcohols, alkanes, lipids, sugars, pigments or terpenes<sup>3-5</sup>. By contrast with land  
52 plant-based photoproduction, microalgae do not compete with agriculture and can be grown  
53 at high yields even at large scale<sup>4, 6</sup>, including on waste streams, thus minimizing inputs<sup>3</sup>. The  
54 green microalga *Chlamydomonas reinhardtii* (referred to hereafter as “Chlamydomonas”) has  
55 been extensively engineered for basic research and industrial biotechnology<sup>4, 6-8</sup>. Its nuclear  
56 and organellar genomes are sequenced and annotated, molecular biology techniques and  
57 culture conditions are highly developed, and its physiology and metabolism are well  
58 understood<sup>9-13</sup>. Moreover, the metabolic plasticity and cellular compartments of  
59 *Chlamydomonas* offer great potential for advanced metabolic engineering strategies<sup>14, 15</sup>.  
60 *Chlamydomonas* has already been engineered for production of the biodiesel precursor  
61 bisabolene<sup>8</sup>, the terpene patchoulol<sup>7</sup>, and recombinant proteins as well as enzymes such as  
62 an HIV antigen<sup>16</sup> and xylanase<sup>17</sup>. Despite these proofs of concept however, engineering of  
63 *Chlamydomonas* is still slow due to a lack of standardized resources and tools<sup>11</sup>. Development  
64 of the field of algal synthetic biology offers the means to enable design and construction of  
65 microalgal cells with defined and predictable properties<sup>18</sup>. Besides biotechnological  
66 applications, the transition from empirical to synthetic approaches also provides the  
67 opportunity to answer fundamental biological questions using new concepts and approaches  
68 based on understanding by construction rather than deconstruction.

69 Synthetic biology approaches, predicated on the Design-Build-Test-Learn cycle<sup>19</sup>, make  
70 organisms easier to engineer through the use of standardized parts and their assembly to  
71 simplify the building of designed DNA molecules<sup>19</sup>. Among available standards<sup>20</sup>, the Golden  
72 Gate Modular Cloning (MoClo) technology, based on Type IIS restriction enzymes, offers  
73 extensive standardization and allows the assembly of complex multigenic DNA from basic  
74 gene parts (*e.g.* promoters, CDS, terminators) in just two steps<sup>21, 22</sup>. The method accelerates  
75 and multiplies the possibilities to permute multiple genetic elements, and makes facile the  
76 building of multigene constructs for full metabolic pathways<sup>23</sup>. MoClo is efficient and versatile,  
77 but relies on intensive upfront generation of a standardized library of basic building blocks,  
78 the gene parts, that have been domesticated to remove Type IIS sites, and codon optimized  
79 for the host as appropriate. MoClo toolkits have already been developed for a few model  
80 organisms<sup>24-29</sup> although not yet for microalgae.

81 Here, we report the generation of a MoClo toolkit composed of more than 100 gene parts  
82 codon-optimized for the *Chlamydomonas* nuclear genome. These genetic parts were designed  
83 to provide maximum modularity to end-users, and to facilitate the development of engineered  
84 strains for fundamental and green biotechnological applications, through iterative design and  
85 testing. We provide functional validation and characterization of many gene parts in several  
86 *Chlamydomonas* strains. This kit is available to the community, to allow *Chlamydomonas* to  
87 become the next chassis for sustainable synthetic biology approaches.

## 88 **RESULTS**

### 89 **Standard and content of the *Chlamydomonas* MoClo kit**

90 Standardization is the key to efficient building. The *Chlamydomonas* MoClo kit adopts the  
91 syntax proposed by the plant synthetic biology community including the OpenPlant

92 Consortium<sup>30</sup> (Fig. 1). This syntax is defined for level 0 plasmids containing standard gene parts  
93 (promoters, coding sequences, untranslated regions, etc.) and assigns strict fusion sites for 10  
94 cloning positions. In a single step, standardized parts can be assembled into modules  
95 (Transcriptional Unit, TU, level 1) and modules into devices (multigenic construct, level M or  
96 2) according to the original MoClo syntax<sup>22</sup> (Supplementary Fig. 1). Our *Chlamydomonas*  
97 MoClo toolkit is composed of a set of 119 parts representing 67 unique genetic elements  
98 available at different positions within the standard, thereby providing maximum modularity  
99 to designers (Fig. 1, Fig. 2). The kit recapitulates most of the standard genetic elements  
100 previously developed for *Chlamydomonas* which we “domesticated” by removing *Bpil* and  
101 *Bsal* restriction sites (the two enzymes used by the MoClo strategy<sup>22</sup>, Supplemental Figure 1)  
102 from their sequences by DNA synthesis or PCR-based mutagenesis. The available gene parts  
103 encompass 7 promoters coupled or not to their original 5’UTR, the corresponding 5’UTR and  
104 the *CrTHI4* riboswitch, 8 immunological or purification tags in positions leading to N- or C-  
105 terminal translational fusions, 9 signal and targeting peptides, 12 reporters, 5 antibiotic  
106 resistance genes, the foot and mouth virus (FMDV) 2A peptide which allows expression of two  
107 or more proteins from a single transcriptional unit<sup>17, 31, 32</sup>, 2 micro RNA (miRNA) backbones  
108 and associated controls, and six 3’UTR-terminators (Fig. 1b, Fig. 2 and Supplementary Table  
109 1). All sequences and plasmids are available through the public Addgene repository  
110 (<http://www.addgene.org/>).

### 111 **Constitutive promoters and reporter genes**

112 Five antibiotic resistance genes are used as selectable markers for *Chlamydomonas* but also  
113 can function as reporter genes<sup>33, 34</sup>. We assembled three modules that allow control of the  
114 expression of the *aadA* gene, conferring spectinomycin resistance, by three constitutive

115 promoters:  $P_{PSAD}$  and  $P_{\beta TUB2}$  with or without the first intron of  $\beta TUB2$  (pCM1-1 to 3,  
116 Supplementary Table 3). The transformation efficiency of the three modules in UVM4<sup>35</sup> cells  
117 was estimated by counting spectinomycin resistant colonies and showed resistance  
118 frequencies within the same range (Fig. 3a). The presence of the first  $\beta TUB2$  intron  
119 significantly increased the transformation efficiency as previously observed with the presence  
120 of  $RBCS2$  introns in the *ble* marker<sup>33, 36, 37</sup>. Alternative reporters are bioluminescent proteins,  
121 which allow more sensitive and quantitative analysis of gene expression. The kit contains  
122 *Gaussia princeps* luciferase, the brightest luciferase established in Chlamydomonas<sup>38</sup>, as well  
123 as the redesigned Nanoluciferase (NanoLuc) which provides a stable and strong luminescence  
124 signal<sup>39</sup>. Chlamydomonas NanoLuc was specifically developed for our MoClo kit through  
125 recoding to match the codon bias of Chlamydomonas, and cloned at 6 different positions  
126 within the standard. This new part was first tested with the most widely used  
127 promoter/terminator combination ( $P_{AR}$  promoter /  $T_{RBCS2}$  terminator) for strong constitutive  
128 expression in Chlamydomonas. The corresponding module (pCM1-04) was assembled with  
129 another module conferring paromomycin resistance (Supplementary Fig. 2) into a device  
130 (pCMM-1) that was introduced into the genome of the D66 strain (CC-4425, Fig. 3b). Among  
131 paromomycin resistant colonies,  $34.8\% \pm 8.3$  (N=48, mean  $\pm$  SEM) were luminescent. The  
132 signal was variable between clones due to genomic position effects<sup>40, 41</sup> but was linear from  
133  $50$  to  $5 \times 10^5$  cells (Fig. 3b and Supplementary Fig. 2). By contrast, non-expressing  
134 transformants (resistant to paromomycin only) or the D66 recipient strain displayed only a  
135 faint signal, 3 orders of magnitude lower, and saturating swiftly (Fig. 3b, inset). The modularity  
136 of the MoClo strategy allows rapid assessment of combinations of multiple parts. For example,  
137 we assembled 4 modules where NanoLuc expression is controlled by all possible combinations  
138 of the two most common constitutive promoters ( $P_{AR}$  and  $P_{PSAD}$ ) and terminators ( $T_{RBCS2}$  and

139  $T_{PSAD}$ ) (Fig. 3b, pCM1-4 to 7, Supplementary Table 3). Each module was assembled with the  
140 paromomycin resistance module (pCMM-1 to 4, Supplementary Table 4) and introduced into  
141 the *Chlamydomonas* genome. Bioluminescence levels were averaged over hundreds of  
142 transformants to account for the genome position effect<sup>40, 41</sup>. The strengths of the two  
143 promoters were found to be comparable, whilst  $T_{PSAD}$  appeared to confer robust expression  
144 from both promoters, 10-fold higher than  $T_{RBCS2}$  (Fig. 3c). In a distinct context (strain, reporter  
145 sequence, culture conditions, etc.), the same genetic element may perform differently<sup>31, 35</sup>.  
146 Such context sensitivity can be overcome by taking advantage of the modularity of the  
147 *Chlamydomonas* MoClo kit, which allows for the rapid characterization of all possible parts  
148 combinations. These results also confirmed the performance of the *Chlamydomonas* NanoLuc  
149 reporter and its employability for detailed understanding and characterization of genetic  
150 circuits especially if coupled with automated cell-sorting microfluidic devices<sup>42</sup>.

### 151 **Control of gene expression**

152 To build genetic circuits, the fine-tuning of gene expression is a prerequisite. Multiple parts  
153 enabling controlled gene expression have therefore been implemented. The activity of the  
154  $P_{NIT1}$  promoter can be controlled by switching the nitrogen source since it is strongly repressed  
155 by ammonium and highly induced on nitrate<sup>34, 43, 44</sup>. A module where  $P_{NIT1}$  controls expression  
156 of the *ble-GFP* gene (pCM1-8) conferred strong zeocin resistance in the CC-1690 strain but  
157 only when ammonium was replaced by nitrate as nitrogen source. By contrast, the  $P_{PSAD}$   
158 promoter (pCM1-9) conferred strong antibiotic resistance on both nitrogen sources (Fig. 4a  
159 and Supplementary Fig. 3a-c). The vitamin B<sub>12</sub>-repressible promoter  $P_{METE}$ <sup>45</sup> allowed  
160 conditional functional complementation of the photosynthetic mutant *nac2-26* (CC-4421),  
161 which lacks photosystem II due to the absence of the TPR-like protein NAC2 required for

162 stability of the *psbD* mRNA encoding the D2 reaction center protein<sup>46</sup>. *nac2-26* mutant cells  
163 engineered with a module harboring the *NAC2* coding sequence under the control of the *P<sub>METE</sub>*  
164 promoter (pCM1-10) could grow photoautotrophically in the absence of vitamin B<sub>12</sub>, but  
165 growth was compromised by increasing its concentration by amounts as low as 5 ng/L (Fig.  
166 4b).

167 Regulation of gene expression can also be controlled by vitamin B<sub>1</sub> (thiamine) at the level of  
168 the transcript through riboswitches<sup>47, 48</sup>. Binding of thiamine pyrophosphate to the *THI4*  
169 riboswitch (RS) results in alternative splicing and retention of an 81 bp upstream open reading  
170 frame, ultimately interfering with translation<sup>47, 48</sup>. The RS also responds when cells are grown  
171 in the presence of the thiamine biosynthetic intermediate 4-methyl-5-(2-hydroxyethyl)  
172 thiazole (HET), but not with 4-amino-5-hydroxymethyl-2-methylpyrimidine (HMP)<sup>47</sup>. A module  
173 combining *P<sub>AR</sub>* and *THI4 (RS)* to drive expression of the *ble-GFP* gene (pCM1-11) conferred  
174 conditional zeocin sensitivity in the UVM4 strain<sup>35</sup>. Resistance was compromised by thiamine  
175 or HET but not HMP (Fig. 4c and Supplementary Fig. 3d), thereby demonstrating the efficient  
176 repression of the transgene through the *THI4* riboswitch.

177 Finally, to allow targeted repression of gene expression, a microRNA precursor sequence  
178 derived from the pre-miR1157 and used for the generation of artificial miRNAs (amiRNA)<sup>49</sup>  
179 was re-designed for compatibility with the Golden Gate cloning method. To demonstrate its  
180 effectiveness in driving gene repression, a specific amiRNA sequence directed against the  
181 *MAA7* gene, whose repression provides resistance to 5'-fluoroindole (5'-FI)<sup>50</sup>, was inserted  
182 into the microRNA precursor. A control random sequence ("scrambled") amiRNA was inserted  
183 into the same backbone. These parts were placed under the control of *P<sub>PSAD</sub>* and *T<sub>PSAD</sub>* (pCM1-  
184 12 and 13) and assembled with a paromomycin resistance module (pCM1-27). The same  
185 amiRNA sequences were introduced into the previously established pChlamiRNA3 vector<sup>49</sup> as



186 controls. After transformation of the CC-1690 strain, 36% of paromomycin-resistant cells  
187 displayed resistance to 5'-FI with the device targeting *MAA7* (pCMM-5) but not with the  
188 scrambled amiRNA (pCMM-6) (Fig. 4d and Supplementary Fig. 3f). A modified 5' rapid  
189 amplification of cDNA ends (5'-RACE) assay revealed that the *MAA7* transcript was most  
190 frequently cleaved at a site corresponding to positions 10 and 11 of the amiRNA, as expected  
191 for a specific action of the miRNA (Fig. 4d). The properties of controllable parts can also be  
192 combined as shown for *P<sub>NIT1</sub>* control of amiRNA-dependent gene repression<sup>34</sup>. An amiRNA  
193 strategy recently proved useful for concerted metabolic engineering of a biodiesel precursor  
194 in *Chlamydomonas*<sup>8</sup>. The versatility of the MoClo kit opens new possibilities for sophisticated  
195 metabolic engineering strategies, *e.g.* the specific downregulation of up to six target genes  
196 with one level M assembly.

#### 197 **Multiple fusion tags for detection and purification of gene products.**

198 Protein fusion tags are indispensable tools used to improve protein expression yields, enable  
199 protein purification, and accelerate the characterization of protein structure and function<sup>51</sup>.  
200 Our MoClo kit includes multiple epitope and affinity tags known to be functional in  
201 *Chlamydomonas*. The modularity of the MoClo assembly allows rapid assessment of the best  
202 tagging strategy through a rapid design/build/test/learn cycle. We took advantage of the well  
203 characterized *rap2* mutant ( $\Delta$ *FKBP12*), which is insensitive to rapamycin<sup>52</sup>, to test the  
204 functionality of five tags (Fig. 5a,b). We designed and built 5 devices allowing strong  
205 constitutive expression of N- or C-terminal tagged FKBP12 coupled to a paromomycin module  
206 (pCMM-7 to 11, Fig. 5c-h and Supplementary Table 4). The engineered strains were selected  
207 on paromomycin and the functionality of the fusion protein was tested by assessing sensitivity  
208 to rapamycin. Protein extracts were probed by immunoblotting using FKBP12-specific and tag-

209 specific antibodies (Fig. 5d-h). All tags allowed detection (Fig. 5d-h) or purification (Fig. 5i) of  
210 FKBP12 even though some were not functional for restoring rapamycin sensitivity. The test  
211 revealed that pCMM-9 outperforms other devices since it provides a WT-like phenotype and  
212 expression level coupled to a strong and specific Myc signal with no significant processing of  
213 the protein. These results demonstrate the importance of the modularity provided by the  
214 Chlamydomonas MoClo toolkit for designing optimal fusion proteins.

### 215 **Visualization and targeting of proteins in living cells**

216 Fluorescent protein tags allow the temporal and spatial monitoring of dynamic expression  
217 patterns at cellular and subcellular scales<sup>53</sup>. Natural and synthetic metabolic pathways can be  
218 optimized through spatial organization since cell compartments offer many advantages, such  
219 as isolation of metabolic reactions and generation of concentration gradients<sup>14</sup>. In a eukaryotic  
220 chassis like Chlamydomonas, organelles such as microbodies, mitochondria and chloroplasts  
221 can be engineered to implement or improve metabolic pathways<sup>15</sup>. The Chlamydomonas  
222 MoClo kit includes 11 targeting and signal peptides that allow the targeting of fusion proteins  
223 to mitochondria, chloroplast, nucleus, secretory pathway, ER and peroxisome-like  
224 microbodies. The functionality of the targeting and signal peptides and of the five fluorescent  
225 proteins (mVenus - yellow, mCherry - red, mRuby2 - red, Clover - green, mCerulean3 - cyan)  
226 included in the toolkit was tested. Eight modules (pCM1-19 to 26, Supplementary Table 3)  
227 combining diverse fluorescent proteins and targeting sequences were assembled into devices  
228 with an antibiotic resistance module (pCMM-12 to 19). All devices were found to behave as  
229 expected and provided the expected fluorescent signal in the targeted compartment (Fig. 6).  
230 The fluorescent and targeting parts of the Chlamydomonas MoClo toolkit, most of which have  
231 been validated here, enable engineering in the third dimension<sup>14</sup> *i.e.* isolation and

232 organization in multiple cellular compartments, and offer new tools for biological  
233 design/build/test cycles.

## 234 **Discussion**

235 The Chlamydomonas MoClo toolkit presented here provides more than 100 domesticated  
236 gene parts to allow advanced synthetic biology in microalgae. Numerous parts of multiple  
237 types have been characterized and validated in different genetic backgrounds<sup>10</sup> and culture  
238 conditions, and can be readily used for biological design without further development. With  
239 the efficiency and modularity of the MoClo strategy, molecular cloning is no longer a limiting  
240 step for engineering Chlamydomonas cells. Indeed, from design to building, a complex device  
241 of up to six different genes/modules can be obtained within a week using the standardized  
242 parts provided in our kit. The modularity will also enable combinatorial assembly by shuffling  
243 part libraries<sup>54</sup> and determine *a posteriori* which combination is the most relevant. The  
244 development of gene-editing technologies in Chlamydomonas, including Zinc-finger  
245 nucleases<sup>55, 56</sup> and several CRISPR-Cas9 approaches<sup>55, 57-59</sup>, together with the development of  
246 high-throughput microfluidics<sup>42</sup> are beginning to gather pace. Coupling these resources to our  
247 standardized MoClo toolkit will facilitate the use of Chlamydomonas as the photosynthetic  
248 chassis for innovative synthetic biology approaches aimed at fundamental and  
249 biotechnological applications. We expect that the creativity of designers, released from the  
250 time constraints associated with classical cloning strategies, will allow rapid expansion of the  
251 standard gene parts, modules and devices through open distribution, notably using the  
252 Addgene repository. We invite the community to openly share their parts through Addgene  
253 and/or our consortium (contact M. Schroda). The development of the Chlamydomonas MoClo  
254 toolkit constitutes a complete step-change in the fields of microalgal biology and

255 biotechnology. The parts developed for the MoClo toolkit may also be employed in other  
256 microalgal species since the orthogonality of several *Chlamydomonas* transcriptional units has  
257 been demonstrated in multiple hosts, including the industrially relevant species *Chlorella*  
258 *ellipsoidea*, *Nannochloropsis sp.* and *Dunaliella salina*<sup>60</sup>. Synthetic approaches will allow  
259 engineering of microalgae in a predictable and efficient manner and thereby offer great  
260 potential to couple environmental protection, energy transition and bioeconomic growth<sup>4</sup>.

261

## 262 **Methods**

263 All chemicals were obtained from Sigma-Aldrich, unless otherwise specified.

264

### 265 ***Escherichia coli* and *Chlamydomonas reinhardtii* strains, transformation and growth** 266 **conditions.**

267 Bacterial growth was performed at 37°C in LB broth supplemented with agar (20% m/V),  
268 spectinomycin (50 µg/mL), ampicillin or carbenicillin (50 or 100 µg/mL, respectively) and X-gal  
269 (40 µg/mL) when required. Chemically competent *E. coli* DH10β (New England Biolabs) were  
270 used for transformation (by heat shock following the manufacturer's instructions) and  
271 maintenance of plasmids. All plasmids of the kit were maintained and amplified in TOP10  
272 *E. coli* strain prior to submission to Addgene.

273 *C. reinhardtii* strains<sup>35, 46, 52, 61, 62</sup>, culture and transformation conditions are recapitulated in  
274 Supplementary Table 5. They were grown in Tris-Acetate-Phosphate (TAP) medium<sup>63</sup>  
275 supplemented with agar (1.6 % m/V), spectinomycin (100 µg/mL), paromomycin (15 µg/mL),  
276 zeocin (ThermoFisher Scientific, 10 to 15 µg/mL), 5-fluoroindole (20 µM) or rapamycin (LC  
277 Laboratories, 1 µM) when required. For *NIT1* promoter characterization (Figure 4a), a  
278 modified TAP medium lacking nitrogen source (TAP-N) was used instead, and was

279 supplemented with 4 mM KNO<sub>3</sub> (nitrate) or 7.5 mM NH<sub>4</sub>Cl (ammonium). For NAC2 autotrophy  
280 test (Figure 4b), cells were grown in minimal media (HSM) for selection of complemented  
281 strains. The responsiveness to B12 was assessed on plate and then in liquid. Cells were grown  
282 for 15 days in HSM until 1-5 x10<sup>7</sup> cells/mL concentration prior to inoculation in a 96-well plate  
283 at a concentration of 10<sup>5</sup> cells/mL in 200 µL of HSM. For response assays (Figure 4c) thiamine  
284 (Melford Laboratories Ltd.), 4-methyl-5-(2-hydroxyethyl) thiazole (HET) and 4-amino-5-  
285 hydroxymethyl-2-methylpyrimidine (HMP, Fluorochem UK) were added to TAP media at a  
286 final concentration of 10 µM.

287 For transformation by electroporation (see Supplementary Table 5), a TAP culture of 1-5 x 10<sup>6</sup>  
288 cells/mL was concentrated 100 times in TAP complemented with 60 mM sucrose or the MAX  
289 Efficiency Transformation reagent for Algae (ThermoFisher scientific) and 25-250 µL were  
290 incubated with 80-300 ng of DNA for 10-30 min on ice in a 0.4 cm gapped cuvette (BioRad)  
291 prior to electroporation (BioRad Gene Pulser Xcell). The cells were then left to recover in TAP  
292 complemented with 40-60 mM sucrose for 16 h under appropriate light and shaking  
293 conditions (typically 50 µmol photon m<sup>-2</sup> s<sup>-1</sup> at 100 rpm) prior to plating on TAP-agar plates  
294 with adapted antibiotics. Transformation by glass-beads method followed previously  
295 published protocols<sup>7, 64</sup>. Briefly, after growth in TAP until 5 x 10<sup>6</sup> cells/mL, cells were  
296 concentrated 30 times and 5 x 10<sup>7</sup> cells were mixed with DNA using glass beads. After 2-fold  
297 dilution with TAP, 2.5 x 10<sup>7</sup> cells were spread onto TAP agar plates containing 100 µg ml<sup>-1</sup>  
298 spectinomycin. Plates were incubated for 16 h in the dark prior to light exposition (30 µmol  
299 photon.m<sup>-2</sup>.s<sup>-1</sup>). When colony counting was performed (Figure 3a), it was 8 days after the  
300 beginning of light. In both cases, the transformation protocol leads to insertion of a linear DNA  
301 in a random location within the nuclear genome.

302

303 **Design.** All *in silico* sequence designs and analysis were performed with Serial Cloner,  
304 Benchling, SnapGene, ApE or Genome Compiler. For exogenous parts, reverse translation was  
305 performed with Serial Cloner using *C. reinhardtii* nuclear genome codon frequency  
306 (<http://www.kazusa.or.jp/codon/cgi-bin/showcodon.cgi?species=3055>).

307 amiRNAs can be generated using DNA parts pCM0-068 and pCM0-069. Both are derived from  
308 the endogenous pre-miR1157<sup>65</sup>, but differ in the way in which the amiRNA specific sequence  
309 is introduced. pCM0-069/pCMM-20 is analogous to pChlamyRNA3<sup>65</sup>, and a dsDNA fragment  
310 containing the amiRNA/loop/amiRNA\* sequence is introduced into a *SpeI* site inside the  
311 miRNA precursor sequence. pCM0-068 presents two divergently oriented *Bpil* sites, allowing  
312 the cloning of the dsDNA fragment by Golden Gate. In this last case, the dsDNA fragment is  
313 formed by the annealing of two oligos with the following sequence: 1) sense oligo (5' AGTA-  
314 (MIRNA\*SEQ)-TCTCGCTGATCGGCACCATGGGGGTGGTGGTGATCAGCGCTA-(MIRNA SEQ)-T 3'),  
315 2) anti-sense oligo (5'CAGT-A-(rev com MIRNA SEQ)-  
316 TAGCGCTGATCACCACCACCCCATGGTGCCGATCAGCGAGA-(rev com MIRNA\*SEQ) 3'). There  
317 are online tools that help with the design of the amiRNA sequence  
318 (<http://wmd3.weigelworld.org/cgi-bin/webapp.cgi>).

319  
320 **Parts repository.** All sequences listed in Supplementary Table 2 were deposited in Addgene.  
321 Physical distribution of the DNA is performed through Addgene. We invite the community to  
322 share their future parts through Addgene and/or with our consortium (contact M. Schroda)  
323 which will make them available to the community.

324  
325 **Parts cloning.** All PCR reactions were performed using the Phusion DNA polymerase, KOD  
326 Xtreme Hot Start DNA polymerase (Merck) or Q5 DNA polymerase purchased from New

327 England Biolabs (NEB) following the manufacturer's instructions adapted to GC-rich DNA,  
328 typically duration of hybridization and polymerization was doubled and/or GC enhancer  
329 solution was used. Molecular biology kits were purchased from Macherey-Nagel, peqLab, NEB  
330 or QIAGEN (gel extraction and miniprep kits). Primers were produced by Eurofins Genomics or  
331 Sigma-Aldrich while synthesized parts were obtained from Genecust, DC Biosciences, IDTDNA  
332 or Sigma-Aldrich.

333

334 **MoClo Assembly Conditions.** All Restriction/ligation reactions were performed using *BbsI* or  
335 *BbsI*-HF (*Bpil* is an isoschizomer) or *BsaI*-HF (NEB or ThermoFisher) together with T4 ligase  
336 (NEB) in a medium containing the NEB CutSmart buffer and 1 mM ATP (with stock of 10 mM  
337 solubilized in 0.1 M Tris-HCl, pH 7.9). Typical ratio between destination plasmid (100 fmol) and  
338 entry plasmid/parts was 1:2. To facilitate handling of the kit for end-users, we provide detailed  
339 protocols and reaction mix calculators for each type of assembly: level 0 for parts  
340 (Supplementary Table 6), level 1 for modules (Supplementary Table 7) and level M for devices  
341 (Supplementary Table 8).

342

343 **Quality Control of generated DNAs.** All plasmids were controlled by differential restriction. In  
344 addition, all level 0 plasmids were sequenced with specific primers. Sequencing was  
345 performed by Eurofins Genomics, Source BioSciences UK, SeqLab, MacroGen, Microsynth,  
346 GATC Biotech or Core Facility (CeBiTec, Bielefeld University).

347

348 **NanoLuc activity determination.** Reagents were purchased from Promega (ref. N1110) and  
349 activity was determined as previously described<sup>39</sup>. For screening, *C. reinhardtii* colonies were  
350 transferred into a 96-well plate containing 100  $\mu$ L of TAP in each well. After gentle

351 resuspension, 50  $\mu$ L was transferred into a solid white 96-well plate to which 50  $\mu$ L of Nano-  
352 Glo substrate diluted in the provided buffer (2% V/V) was added and gently mixed by pipetting.  
353 Luminescence was measured at 460 nm with a CLARIOstar plate reader (BMG Labtech). For  
354 promoter/terminator combination assessment experiment (Figure 3c), all *C. reinhardtii*  
355 colonies from a transformation event were pooled and resuspended in TE buffer (50 mM Tris-  
356 HCl pH 7.9, 1 mM EDTA) complemented with anti-protease (1 tablet per 50 mL, Sigma-Aldrich:  
357 S8830). The cells were lysed by vortexing 10 seconds twice in the presence of glass beads  
358 (about 1:5 ratio beads/cells V/V) prior to two centrifugations (20000 g for 10 min at 4°C) to  
359 clarify the supernatant. The protein concentration was then determined using Bradford  
360 reagent with a Bovine Serum Albumin standard curve and the concentration was standardized  
361 to 0.5 g/L. The activity was determined in a 96-well plate in a final volume of 50  $\mu$ L (1:1 with  
362 nano-Glo resuspended in provided lysis buffer) per well. NanoLuc activity was determined on  
363 6 different increasing protein quantities (0.1 to 2.5  $\mu$ g) for each assay, allowing to assess  
364 linearity of the signal.

365

#### 366 **Absorbance measurement of cultures growing in microtiter plates**

367 Growth in microtiter plates was determined by measuring the optical density of each well at  
368 730 nm. Microtiter plates containing 180-200  $\mu$ L culture were incubated under constant light  
369 ( $125 \mu\text{mol photon}\cdot\text{m}^{-2}\cdot\text{s}^{-1}$ ) at 25°C and 40 rpm orbital shaking. For density determination,  
370 cultures were resuspended by pipetting and 100  $\mu$ L of cell suspension was transferred to a  
371 new microtiter plate containing 50  $\mu$ L TAP 0.03% Tween-20. Optical density of each well was  
372 determined at 730 nm in a CLARIOstar plate reader (BMG Labtech). Plates were shaken for 6-  
373 10 sec at 600 rpm before measurement.

374



375 **RNA extraction and miRNA-mediated cleavage mapping**

376 RNA isolation was carried out as previously described<sup>49</sup> (a detailed protocol can be found at  
377 <http://www.plantsci.cam.ac.uk/research/davidbaulcombe/methods/downloads/smallrna.pdf>  
378 [f/view](#)), with the following modifications: Cells were centrifuged and resuspended in 0.25 mL  
379 of water and mixed with 0.25 mL Lysis buffer (50 mM Tris-HCl pH 8.0, 200 mM NaCl, 50 mM  
380 EDTA, 2% SDS, 1 mg/mL proteinase K). Lysis buffer was incubated at 50°C for 5 min prior mixing  
381 with cells. Cell suspension was then incubated at 25°C for 20 min. Finally, 2 mL of PureZol  
382 (Biorad) was added and samples were snap-frozen. RNA quality was assessed in gel and  
383 quantified in Nanodrop (ThermoFisher scientific).

384 miRNA cleavage site determination was performed as previously described<sup>66</sup>. Briefly, 10 µg of  
385 total RNA was ligated with an RNA oligo (5' CGACUGGAGCACGAGGACACUGACAUGGAC  
386 UGAAGGAGUAGAAA 3') using T4 RNA ligase for 1 h at 37°C. RNA was extracted with  
387 phenol:chloroform and precipitated with ethanol and sodium acetate. The precipitated RNA was  
388 retrotranscribed into cDNA by SuperScript IV reverse transcriptase (ThermoFisher scientific),  
389 using random hexamers and following manufacturer's recommendations. Two µL of the cDNA  
390 was used as template of a PCR using primers FJN456 (5'- CGACTGGAGCACGAGGACACTGA) and  
391 FJN495 (5'- TGGGGTAGGGGTGGGGGCCAG). Two µL of this PCR was used as template of a  
392 second PCR with primers FJN457 (5'- GGACACTGACATGGACTGAAGGAGTA) and FJN496 (5'-  
393 TGACCCAGTCGCGGATGGCCT). PCR was resolved in a 2% agarose gel and the specific band was  
394 isolated from the gel and cloned into pGEM-T easy (Promega) for sequencing.

395

396 **Immuno-blotting.** Chlamydomonas cells expressing FKB12 fusion proteins from liquid cultures  
397 were collected by centrifugation 4000 g for 5 min at room temperature (RT), washed in 50 mM  
398 Tris-HCl pH 7.5, and resuspended in a minimal volume of the same solution. Cells were lysed

399 by two cycles of slow freezing to -80°C followed by thawing at RT. The soluble cell extract was  
400 separated from the insoluble fraction by centrifugation (15000 g for 20 min at 4°C). Total  
401 protein extracts (15 µg) were then subjected to 15% SDS-PAGE.

402 mCherry-expressing cells were harvested at 3500 rpm for 2 min (4 °C) and resuspended in  
403 60 µL of DTT-carbonate buffer (0.1 M DTT, 0.1 M Na<sub>2</sub>CO<sub>3</sub>). After freezing at -20 °C and thawing,  
404 55 µL of SDS-Sucrose buffer were added (5 % SDS, 30 % sucrose). Samples were then boiled  
405 for 45 s at 95 °C, followed by 2 min incubation on ice and 13000 g centrifugation for 2 min at  
406 RT. Protein extracts corresponding to 2 µg of Chlorophyll were then separated using 12% SDS-  
407 PAGE.

408 For immunoblot analyses, proteins were then transferred to nitrocellulose membranes (Bio-  
409 Rad, 162-0115 or Amersham Protran). After blocking with 3 to 5% low-fat Milk in PBS for 1 h  
410 at RT, membranes were incubated with primary antibody in 5% low-fat Milk in PBS for 16 h at  
411 4°C. After 4 washes in PBS - 0.1% tween-20 (TPBS), the membranes were incubated with  
412 secondary antibody in 5% low-fat Milk in PBS for 1 h at RT, and subsequently washed 4 time  
413 in TPBS prior to chemi-luminescence revelation using ECL. Primary antibodies used were anti-  
414 FKBP12<sup>52</sup> (1/5000 dilution; secondary was anti-rabbit 1/10000), anti-FLAG (Sigma-Aldrich  
415 F1804, 1/5000 dilution; secondary was anti-mouse 1/5000), anti-STREP (IBA, Catalog N. 2-  
416 1509-001, 1/5000 dilution; conjugated to HRP), anti-cMYC (Sigma-Aldrich M4439, 1/2500  
417 dilution; secondary was anti-mouse 1/5000), anti-HA (Sigma-Aldrich H9658, 1/5000 dilution;  
418 secondary was anti-mouse 1/2500) and anti-PRPL1<sup>67</sup>. For mCherry serum, rabbits were  
419 immunized against purified full-length mCherry protein containing an N-terminal His<sub>6</sub>-tag.

420

421 **Microscopy.** For mCherry experiments (Figure 6b-e), images were taken at 100x magnification  
422 with a BX53F microscope (Olympus). Fluorescence images for the detection of mCherry were

423 taken using a TRITC filter. For other fluorescent proteins (Figure 6f-h), microscopy was  
424 performed as previously described<sup>7, 68</sup>.

425

426 **Accession numbers.** All parts accession numbers and the corresponding references are listed  
427 in Supplementary Table 2.

428

## 429 **ASSOCIATED CONTENT**

### 430 **Supporting Information.**

431 Supplementary Figure 1 - MoClo assembly workflow reflecting the abstraction hierarchy

432 Supplementary Figure 2 - Variability of Nanoluc expression in pCMM-1 transformants.

433 Supplementary Figure 3 - Control of gene expression, complementary data.

434 Supplementary Table 1 - list of all unique parts of the Chlamy MoClo kit

435 Supplementary Table 2 - list of all parts of the Chlamy MoClo kit: level 0 plasmids

436 Supplementary Table 3 - list of all modules used for the Chlamy MoClo kit validation: level 1  
437 plasmids

438 Supplementary Table 4 - list of all modules used for the Chlamy MoClo kit validation: level M  
439 plasmids

440 Supplementary Table 5 - list of Chlamydomonas reinhardtii strains and associated  
441 transformations

442 Supplementary Table 6 - level 0 ligation file: protocol and reaction mix calculator to clone  
443 parts.

444 Supplementary Table 7 - level 1 ligation file: protocol and reaction mix calculator to assemble  
445 modules.

446 Supplementary Table 8 - level M ligation file: protocol and reaction mix calculator to assemble  
447 devices.

448

### 449 **Abbreviation.**

450 MoClo: Modular Cloning, TU: Transcriptional Unit, RBCS2: Ribulose Bisphosphate

451 Carboxylase oxygenase Small subunit 2, HSP70: Heat Shock Protein 70, AR: HSP70A/RBCS2,

452 TUB2: Tubulin 2, PSAD: Photosystem I reaction center subunit II, HET: 4-methyl-5-(2-  
453 hydroxyethyl) thiazole, HMP: 4-amino-5-hydroxymethyl-2-methylpyrimidine, amiRNA:  
454 artificial micro RNA, TAP: Tris Acetate Phosphate

455

456 **Author Information.**

457 K. Vavitsas current address is: Australian Institute for Bioengineering and Nanotechnology  
458 (AIBN), The University of Queensland, Australia

459

460 **Author Contribution.**

461 SDL, AGS, MS, PEJ, OK, JLC and GP created the consortium that led this study.

462 PC, FJN, FW, PM, DCB, GP, JLC, OK, PEJ, MS, AGS and SDL designed the study and wrote the  
463 manuscript.

464 PC, FJN, FW, PM, KB, KJL, MEPP, PA, AGR, SSG, JN, BS, JT, RT, LW, KV, TB, KS, MC, FdC, AD,  
465 MdM, JH, WH, CHM designed parts, modules and devices, performed the experiments, and/or  
466 analyzed data.

467

468 **Competing Financial Interests statement.**

469 The authors declare no competing financial interest.

470

471 **Acknowledgments.**

472 The authors would like to thank Karin Gries and Vincent Assoun for their technical help.

473 This work was supported in part by Agence Nationale de la Recherche Grant ANR-17-CE05-  
474 0008 and LABEX DYNAMO ANR-LABX-011 (to PC, AD, FdC, JH, CHM, MdM, KS, MC and SDL),  
475 by the DFG-funded TRR175 and FOR2092 (to FW, BS, JN, JT, LW, RT and MS), by OpenPlant

476 (BBSRC/EPSRC) (to FJN and SSG), by Ministerio de Economía y Competitividad grants  
477 BFU2015-68216-P and BIO2015-74432-JIN (to JLC and MEPP), by the VILLUM Foundation  
478 (Project no. 13363) (to PEJ, KB, KV), by the Technology Platforms at the Center for  
479 Biotechnology (CeBiTec) Bielefeld University (to KL, TB, and OK), by UK Biotechnology and  
480 Biological Sciences Research Council (BBSRC) (to PM and AGR) and by ERA-SynBio project  
481 Sun2Chem (to PA and GP).

482

### 483 REFERENCES.

- 484 (1) Zargar, A., Bailey, C. B., Haushalter, R. W., Eiben, C. B., Katz, L., and Keasling, J. D. (2017)  
485 Leveraging microbial biosynthetic pathways for the generation of 'drop-in' biofuels, *Curr*  
486 *Opin Biotechnol* 45, 156-163.
- 487 (2) Georgianna, D. R., and Mayfield, S. P. (2012) Exploiting diversity and synthetic biology for the  
488 production of algal biofuels, *Nature* 488, 329-335.
- 489 (3) Wijffels, R. H., Kruse, O., and Hellingwerf, K. J. (2013) Potential of industrial biotechnology with  
490 cyanobacteria and eukaryotic microalgae, *Curr Opin Biotechnol* 24, 405-413.
- 491 (4) Gimpel, J. A., Henríquez, V., and Mayfield, S. P. (2015) In Metabolic Engineering of Eukaryotic  
492 Microalgae: Potential and Challenges Come with Great Diversity, *Front Microbiol* 6.
- 493 (5) Scranton, M. A., Ostrand, J. T., Fields, F. J., and Mayfield, S. P. (2015) Chlamydomonas as a model  
494 for biofuels and bio-products production, *Plant J* 82, 523-531.
- 495 (6) Gangl, D., Zedler, J. A., Rajakumar, P. D., Martinez, E. M., Riseley, A., Wlodarczyk, A., Purton, S.,  
496 Sakuragi, Y., Howe, C. J., Jensen, P. E., and Robinson, C. (2015) Biotechnological exploitation  
497 of microalgae, *J Exp Bot* 66, 6975-6990.
- 498 (7) Lauersen, K. J., Baier, T., Wichmann, J., Wordenweber, R., Mussnug, J. H., Hubner, W., Huser, T.,  
499 and Kruse, O. (2016) Efficient phototrophic production of a high-value sesquiterpenoid from  
500 the eukaryotic microalga *Chlamydomonas reinhardtii*, *Metab Eng* 38, 331-343.
- 501 (8) Wichmann, J., Baier, T., Wentnagel, E., Lauersen, K. J., and Kruse, O. (2017) Tailored carbon  
502 partitioning for phototrophic production of (E)-alpha-bisabolene from the green microalga  
503 *Chlamydomonas reinhardtii*, *Metab Eng*.
- 504 (9) Merchant, S. S., Prochnik, S. E., Vallon, O., Harris, E. H., Karpowicz, S. J., Witman, G. B., Terry, A.,  
505 Salamov, A., Fritz-Laylin, L. K., Marechal-Drouard, L., Marshall, W. F., Qu, L. H., Nelson, D. R.,  
506 Sanderfoot, A. A., Spalding, M. H., Kapitonov, V. V., Ren, Q., Ferris, P., Lindquist, E., Shapiro,  
507 H., Lucas, S. M., Grimwood, J., Schmutz, J., Cardol, P., Cerutti, H., Chanfreau, G., Chen, C. L.,  
508 Cognat, V., Croft, M. T., Dent, R., Dutcher, S., Fernandez, E., Fukuzawa, H., Gonzalez-Ballester,  
509 D., Gonzalez-Halphen, D., Hallmann, A., Hanikenne, M., Hippler, M., Inwood, W., Jabbari, K.,  
510 Kalanon, M., Kuras, R., Lefebvre, P. A., Lemaire, S. D., Lobanov, A. V., Lohr, M., Manuell, A.,  
511 Meier, I., Mets, L., Mittag, M., Mittelmeier, T., Moroney, J. V., Moseley, J., Napoli, C.,  
512 Nedelcu, A. M., Niyogi, K., Novoselov, S. V., Paulsen, I. T., Pazour, G., Purton, S., Ral, J. P.,  
513 Riano-Pachon, D. M., Riekhof, W., Rymarquis, L., Schroda, M., Stern, D., Umen, J., Willows, R.,  
514 Wilson, N., Zimmer, S. L., Allmer, J., Balk, J., Bisova, K., Chen, C. J., Elias, M., Gendler, K.,  
515 Hauser, C., Lamb, M. R., Ledford, H., Long, J. C., Minagawa, J., Page, M. D., Pan, J.,  
516 Pootakham, W., Roje, S., Rose, A., Stahlberg, E., Terauchi, A. M., Yang, P., Ball, S., Bowler, C.,  
517 Dieckmann, C. L., Gladyshev, V. N., Green, P., Jorgensen, R., Mayfield, S., Mueller-Roeber, B.,  
518 Rajamani, S., Sayre, R. T., Brokstein, P., Dubchak, I., Goodstein, D., Hornick, L., Huang, Y. W.,

519 Jhaveri, J., Luo, Y., Martinez, D., Ngau, W. C., Otilar, B., Poliakov, A., Porter, A., Szajkowski, L.,  
520 Werner, G., Zhou, K., Grigoriev, I. V., Rokhsar, D. S., and Grossman, A. R. (2007) The  
521 Chlamydomonas genome reveals the evolution of key animal and plant functions, *Science*  
522 *318*, 245-250.

523 (10) Gallaher, S. D., Fitz-Gibbon, S. T., Glaesener, A. G., Pellegrini, M., and Merchant, S. S. (2015)  
524 Chlamydomonas Genome Resource for Laboratory Strains Reveals a Mosaic of Sequence  
525 Variation, Identifies True Strain Histories, and Enables Strain-Specific Studies, *Plant Cell* *27*,  
526 2335-2352.

527 (11) Scaife, M. A., Nguyen, G. T., Rico, J., Lambert, D., Helliwell, K. E., and Smith, A. G. (2015)  
528 Establishing Chlamydomonas reinhardtii as an industrial biotechnology host, *Plant J* *82*, 532-  
529 546.

530 (12) Li, X., Zhang, R., Patena, W., Gang, S. S., Blum, S. R., Ivanova, N., Yue, R., Robertson, J. M.,  
531 Lefebvre, P. A., Fitz-Gibbon, S. T., Grossman, A. R., and Jonikas, M. C. (2016) An Indexed,  
532 Mapped Mutant Library Enables Reverse Genetics Studies of Biological Processes in  
533 Chlamydomonas reinhardtii, *Plant Cell* *28*, 367-387.

534 (13) Jinkerson, R. E., and Jonikas, M. C. (2015) Molecular techniques to interrogate and edit the  
535 Chlamydomonas nuclear genome, *Plant J* *82*, 393-412.

536 (14) Agapakis, C. M., Boyle, P. M., and Silver, P. A. (2012) Natural strategies for the spatial  
537 optimization of metabolism in synthetic biology, *Nat Chem Biol* *8*, 527-535.

538 (15) Chen, A. H., and Silver, P. A. (2012) Designing biological compartmentalization, *Trends Cell Biol*  
539 *22*, 662-670.

540 (16) Barahimipour, R., Neupert, J., and Bock, R. (2016) Efficient expression of nuclear transgenes in  
541 the green alga Chlamydomonas: synthesis of an HIV antigen and development of a new  
542 selectable marker, *Plant Mol Biol* *90*, 403-418.

543 (17) Rasala, B. A., Lee, P. A., Shen, Z., Briggs, S. P., Mendez, M., and Mayfield, S. P. (2012) Robust  
544 expression and secretion of Xylanase1 in Chlamydomonas reinhardtii by fusion to a selection  
545 gene and processing with the FMDV 2A peptide, *PLoS One* *7*, e43349.

546 (18) Scaife, M. A., and Smith, A. G. (2016) Towards developing algal synthetic biology, *Biochem Soc*  
547 *Trans* *44*, 716-722.

548 (19) Endy, D. (2011) Building a new biology, *C R Chim* *14*, 424-428.

549 (20) Casini, A., Storch, M., Baldwin, G. S., and Ellis, T. (2015) Bricks and blueprints: methods and  
550 standards for DNA assembly, *Nat Rev Mol Cell Biol* *16*, 568-576.

551 (21) Engler, C., Kandzia, R., and Marillonnet, S. (2008) A one pot, one step, precision cloning method  
552 with high throughput capability, *PLoS One* *3*, e3647.

553 (22) Weber, E., Engler, C., Gruetzner, R., Werner, S., and Marillonnet, S. (2011) A modular cloning  
554 system for standardized assembly of multigene constructs, *PLoS One* *6*, e16765.

555 (23) Smanski, M. J., Bhatia, S., Zhao, D., Park, Y., L, B. A. W., Giannoukos, G., Ciulla, D., Busby, M.,  
556 Calderon, J., Nicol, R., Gordon, D. B., Densmore, D., and Voigt, C. A. (2014) Functional  
557 optimization of gene clusters by combinatorial design and assembly, *Nat Biotechnol* *32*,  
558 1241-1249.

559 (24) Celinska, E., Ledesma-Amaro, R., Larroude, M., Rossignol, T., Pauthenier, C., and Nicaud, J. M.  
560 (2017) Golden Gate Assembly system dedicated to complex pathway manipulation in  
561 *Yarrowia lipolytica*, *Microb Biotechnol* *10*, 450-455.

562 (25) Engler, C., Youles, M., Gruetzner, R., Ehnert, T. M., Werner, S., Jones, J. D., Patron, N. J., and  
563 Marillonnet, S. (2014) A golden gate modular cloning toolbox for plants, *ACS Synth Biol* *3*,  
564 839-843.

565 (26) Iverson, S. V., Haddock, T. L., Beal, J., and Densmore, D. M. (2016) CIDAR MoClo: Improved  
566 MoClo Assembly Standard and New E. coli Part Library Enable Rapid Combinatorial Design for  
567 Synthetic and Traditional Biology, *ACS Synth Biol* *5*, 99-103.

568 (27) Lee, M. E., DeLoache, W. C., Cervantes, B., and Dueber, J. E. (2015) A Highly Characterized Yeast  
569 Toolkit for Modular, Multipart Assembly, *ACS Synth Biol* *4*, 975-986.

- 570 (28) Martella, A., Matjusaitis, M., Auxillos, J., Pollard, S. M., and Cai, Y. (2017) EMMA: An Extensible  
571 Mammalian Modular Assembly Toolkit for the Rapid Design and Production of Diverse  
572 Expression Vectors, *ACS Synth Biol*.
- 573 (29) Moore, S. J., Lai, H. E., Kelwick, R. J., Chee, S. M., Bell, D. J., Polizzi, K. M., and Freemont, P. S.  
574 (2016) EcoFlex: A Multifunctional MoClo Kit for E. coli Synthetic Biology, *ACS Synth Biol* 5,  
575 1059-1069.
- 576 (30) Patron, N. J., Orzaez, D., Marillonnet, S., Warzecha, H., Matthewman, C., Youles, M., Raitskin, O.,  
577 Leveau, A., Farre, G., Rogers, C., Smith, A., Hibberd, J., Webb, A. A., Locke, J., Schornack, S.,  
578 Ajioka, J., Baulcombe, D. C., Zipfel, C., Kamoun, S., Jones, J. D., Kuhn, H., Robatzek, S., Van  
579 Esse, H. P., Sanders, D., Oldroyd, G., Martin, C., Field, R., O'Connor, S., Fox, S., Wulff, B.,  
580 Miller, B., Breakspear, A., Radhakrishnan, G., Delaux, P. M., Loque, D., Granell, A., Tissier, A.,  
581 Shih, P., Brutnell, T. P., Quick, W. P., Rischer, H., Fraser, P. D., Aharoni, A., Raines, C., South, P.  
582 F., Ane, J. M., Hamberger, B. R., Langdale, J., Stougaard, J., Bouwmeester, H., Udvardi, M.,  
583 Murray, J. A., Ntoukakis, V., Schafer, P., Denby, K., Edwards, K. J., Osbourn, A., and Haseloff, J.  
584 (2015) Standards for plant synthetic biology: a common syntax for exchange of DNA parts,  
585 *New Phytol* 208, 13-19.
- 586 (31) Lopez-Paz, C., Liu, D., Geng, S., and Umen, J. G. (2017) Identification of Chlamydomonas  
587 reinhardtii endogenous genic flanking sequences for improved transgene expression, *Plant J*  
588 92, 1232-1244.
- 589 (32) Plucinak, T. M., Horken, K. M., Jiang, W., Fostvedt, J., Nguyen, S. T., and Weeks, D. P. (2015)  
590 Improved and versatile viral 2A platforms for dependable and inducible high-level expression  
591 of dicistronic nuclear genes in Chlamydomonas reinhardtii, *Plant J* 82, 717-729.
- 592 (33) Lumberras, V., Stevens, D. R., and Purton, S. (1998) Efficient foreign gene expression in  
593 Chlamydomonas reinhardtii mediated by an endogenous intron, *Plant J* 14, 441-447.
- 594 (34) Strenkert, D., Schmollinger, S., and Schroda, M. (2013) Heat shock factor 1 counteracts  
595 epigenetic silencing of nuclear transgenes in Chlamydomonas reinhardtii, *Nucleic Acids Res*  
596 41, 5273-5289.
- 597 (35) Neupert, J., Karcher, D., and Bock, R. (2009) Generation of Chlamydomonas strains that  
598 efficiently express nuclear transgenes, *Plant J* 57, 1140-1150.
- 599 (36) Schroda, M., Beck, C. F., and Vallon, O. (2002) Sequence elements within an HSP70 promoter  
600 counteract transcriptional transgene silencing in Chlamydomonas, *Plant J* 31, 445-455.
- 601 (37) Eichler-Stahlberg, A., Weisheit, W., Ruecker, O., and Heitzer, M. (2009) Strategies to facilitate  
602 transgene expression in Chlamydomonas reinhardtii, *Planta* 229, 873-883.
- 603 (38) Shao, N., and Bock, R. (2008) A codon-optimized luciferase from *Gaussia princeps* facilitates the  
604 in vivo monitoring of gene expression in the model alga Chlamydomonas reinhardtii, *Curr*  
605 *Genet* 53, 381-388.
- 606 (39) Hall, M. P., Unch, J., Binkowski, B. F., Valley, M. P., Butler, B. L., Wood, M. G., Otto, P.,  
607 Zimmerman, K., Vidugiris, G., Machleidt, T., Robers, M. B., Benink, H. A., Eggers, C. T., Slater,  
608 M. R., Meisenheimer, P. L., Klaubert, D. H., Fan, F., Encell, L. P., and Wood, K. V. (2012)  
609 Engineered luciferase reporter from a deep sea shrimp utilizing a novel imidazopyrazinone  
610 substrate, *ACS Chem Biol* 7, 1848-1857.
- 611 (40) Lodha, M., Schulz-Raffelt, M., and Schroda, M. (2008) A new assay for promoter analysis in  
612 Chlamydomonas reveals roles for heat shock elements and the TATA box in HSP70A  
613 promoter-mediated activation of transgene expression, *Eukaryot Cell* 7, 172-176.
- 614 (41) Barahimipour, R., Strenkert, D., Neupert, J., Schroda, M., Merchant, S. S., and Bock, R. (2015)  
615 Dissecting the contributions of GC content and codon usage to gene expression in the model  
616 alga Chlamydomonas reinhardtii, *Plant J* 84, 704-717.
- 617 (42) Best, R. J., Lyczakowski, J. J., Abalde-Cela, S., Yu, Z., Abell, C., and Smith, A. G. (2016) Label-Free  
618 Analysis and Sorting of Microalgae and Cyanobacteria in Microdroplets by Intrinsic  
619 Chlorophyll Fluorescence for the Identification of Fast Growing Strains, *Anal Chem* 88, 10445-  
620 10451.

- 621 (43) Ohresser, M., Matagne, R. F., and Loppes, R. (1997) Expression of the arylsulphatase reporter  
622 gene under the control of the nit1 promoter in *Chlamydomonas reinhardtii*, *Curr Genet* 31,  
623 264-271.
- 624 (44) Schmollinger, S., Strenkert, D., and Schroda, M. (2010) An inducible artificial microRNA system  
625 for *Chlamydomonas reinhardtii* confirms a key role for heat shock factor 1 in regulating  
626 thermotolerance, *Curr Genet* 56, 383-389.
- 627 (45) Helliwell, K. E., Scaife, M. A., Sasso, S., Araujo, A. P., Purton, S., and Smith, A. G. (2014)  
628 Unraveling vitamin B12-responsive gene regulation in algae, *Plant Physiol* 165, 388-397.
- 629 (46) Boudreau, E., Nickelsen, J., Lemaire, S. D., Ossenbuhl, F., and Rochaix, J. D. (2000) The Nac2 gene  
630 of *Chlamydomonas* encodes a chloroplast TPR-like protein involved in psbD mRNA stability,  
631 *EMBO J* 19, 3366-3376.
- 632 (47) Croft, M. T., Moulin, M., Webb, M. E., and Smith, A. G. (2007) Thiamine biosynthesis in algae is  
633 regulated by riboswitches, *Proc Natl Acad Sci U S A* 104, 20770-20775.
- 634 (48) Moulin, M., Nguyen, G. T., Scaife, M. A., Smith, A. G., and Fitzpatrick, T. B. (2013) Analysis of  
635 *Chlamydomonas* thiamin metabolism in vivo reveals riboswitch plasticity, *Proc Natl Acad Sci*  
636 *U S A* 110, 14622-14627.
- 637 (49) Molnar, A., Schwach, F., Studholme, D. J., Thuenemann, E. C., and Baulcombe, D. C. (2007)  
638 miRNAs control gene expression in the single-cell alga *Chlamydomonas reinhardtii*, *Nature*  
639 447, 1126-1129.
- 640 (50) Palombella, A. L., and Dutcher, S. K. (1998) Identification of the gene encoding the tryptophan  
641 synthase beta-subunit from *Chlamydomonas reinhardtii*, *Plant Physiol* 117, 455-464.
- 642 (51) Young, C. L., Britton, Z. T., and Robinson, A. S. (2012) Recombinant protein expression and  
643 purification: a comprehensive review of affinity tags and microbial applications, *Biotechnol J*  
644 7, 620-634.
- 645 (52) Crespo, J. L., Diaz-Troya, S., and Florencio, F. J. (2005) Inhibition of target of rapamycin signaling  
646 by rapamycin in the unicellular green alga *Chlamydomonas reinhardtii*, *Plant Physiol* 139,  
647 1736-1749.
- 648 (53) Crivat, G., and Taraska, J. W. (2012) Imaging proteins inside cells with fluorescent tags, *Trends*  
649 *Biotechnol* 30, 8-16.
- 650 (54) Engler, C., Gruetzner, R., Kandzia, R., and Marillonnet, S. (2009) Golden gate shuffling: a one-pot  
651 DNA shuffling method based on type IIs restriction enzymes, *PLoS One* 4, e5553.
- 652 (55) Greiner, A., Kelterborn, S., Evers, H., Kreimer, G., Sizova, I., and Hegemann, P. (2017) Targeting of  
653 Photoreceptor Genes in *Chlamydomonas reinhardtii* via Zinc-finger Nucleases and  
654 CRISPR/Cas9, *Plant Cell*.
- 655 (56) Sizova, I., Greiner, A., Awasthi, M., Kateriya, S., and Hegemann, P. (2013) Nuclear gene targeting  
656 in *Chlamydomonas* using engineered zinc-finger nucleases, *Plant J* 73, 873-882.
- 657 (57) Shin, S. E., Lim, J. M., Koh, H. G., Kim, E. K., Kang, N. K., Jeon, S., Kwon, S., Shin, W. S., Lee, B.,  
658 Hwangbo, K., Kim, J., Ye, S. H., Yun, J. Y., Seo, H., Oh, H. M., Kim, K. J., Kim, J. S., Jeong, W. J.,  
659 Chang, Y. K., and Jeong, B. R. (2016) CRISPR/Cas9-induced knockout and knock-in mutations  
660 in *Chlamydomonas reinhardtii*, *Sci Rep* 6, 27810.
- 661 (58) Baek, K., Kim, D. H., Jeong, J., Sim, S. J., Melis, A., Kim, J. S., Jin, E., and Bae, S. (2016) DNA-free  
662 two-gene knockout in *Chlamydomonas reinhardtii* via CRISPR-Cas9 ribonucleoproteins, *Sci*  
663 *Rep* 6, 30620.
- 664 (59) Ferenczi, A., Pyott, D. E., Xipnitou, A., and Molnar, A. (2017) Efficient targeted DNA editing and  
665 replacement in *Chlamydomonas reinhardtii* using Cpf1 ribonucleoproteins and single-  
666 stranded DNA, *Proc Natl Acad Sci U S A* 114, 13567-13572.
- 667 (60) Doron, L., Segal, N., and Shapira, M. (2016) Transgene Expression in Microalgae-From Tools to  
668 Applications, *Front Plant Sci* 7, 505.
- 669 (61) Sager, R. (1955) Inheritance in the Green Alga *Chlamydomonas Reinhardi*, *Genetics* 40, 476-489.
- 670 (62) Kuchka, M. R., Goldschmidt-Clermont, M., van Dillewijn, J., and Rochaix, J. D. (1989) Mutation at  
671 the *Chlamydomonas* nuclear NAC2 locus specifically affects stability of the chloroplast psbD  
672 transcript encoding polypeptide D2 of PS II, *Cell* 58, 869-876.



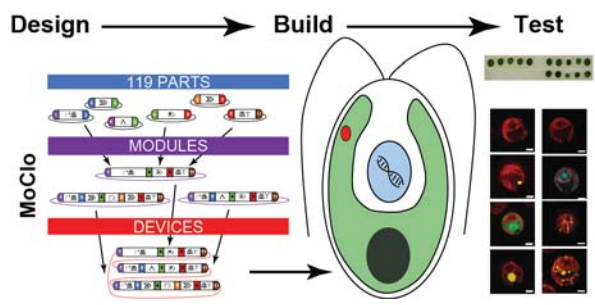
- 673 (63) Gorman, D. S., and Levine, R. P. (1965) Cytochrome f and plastocyanin: their sequence in the  
674 photosynthetic electron transport chain of *Chlamydomonas reinhardi*, *Proc Natl Acad Sci U S*  
675 *A 54*, 1665-1669.
- 676 (64) Kindle, K. L. (1990) High-frequency nuclear transformation of *Chlamydomonas reinhardtii*, *Proc*  
677 *Natl Acad Sci U S A 87*, 1228-1232.
- 678 (65) Molnar, A., Bassett, A., Thuenemann, E., Schwach, F., Karkare, S., Ossowski, S., Weigel, D., and  
679 Baulcombe, D. (2009) Highly specific gene silencing by artificial microRNAs in the unicellular  
680 alga *Chlamydomonas reinhardtii*, *Plant J 58*, 165-174.
- 681 (66) Llave, C., Xie, Z., Kasschau, K. D., and Carrington, J. C. (2002) Cleavage of Scarecrow-like mRNA  
682 targets directed by a class of Arabidopsis miRNA, *Science 297*, 2053-2056.
- 683 (67) Ries, F., Carius, Y., Rohr, M., Gries, K., Keller, S., Lancaster, C. R. D., and Willmund, F. (2017)  
684 Structural and molecular comparison of bacterial and eukaryotic trigger factors, *Sci Rep 7*,  
685 10680.
- 686 (68) Lauersen, K. J., Kruse, O., and Mussnug, J. H. (2015) Targeted expression of nuclear transgenes  
687 in *Chlamydomonas reinhardtii* with a versatile, modular vector toolkit, *Appl Microbiol*  
688 *Biotechnol 99*, 3491-3503.
- 689 (69) Roehner, N., Beal, J., Clancy, K., Bartley, B., Misirli, G., Grunberg, R., Oberortner, E., Pocock, M.,  
690 Bissell, M., Madsen, C., Nguyen, T., Zhang, M., Zhang, Z., Zundel, Z., Densmore, D., Gennari, J.  
691 H., Wipat, A., Sauro, H. M., and Myers, C. J. (2016) Sharing Structure and Function in  
692 Biological Design with SBOL 2.0, *ACS Synth Biol 5*, 498-506.

693

694

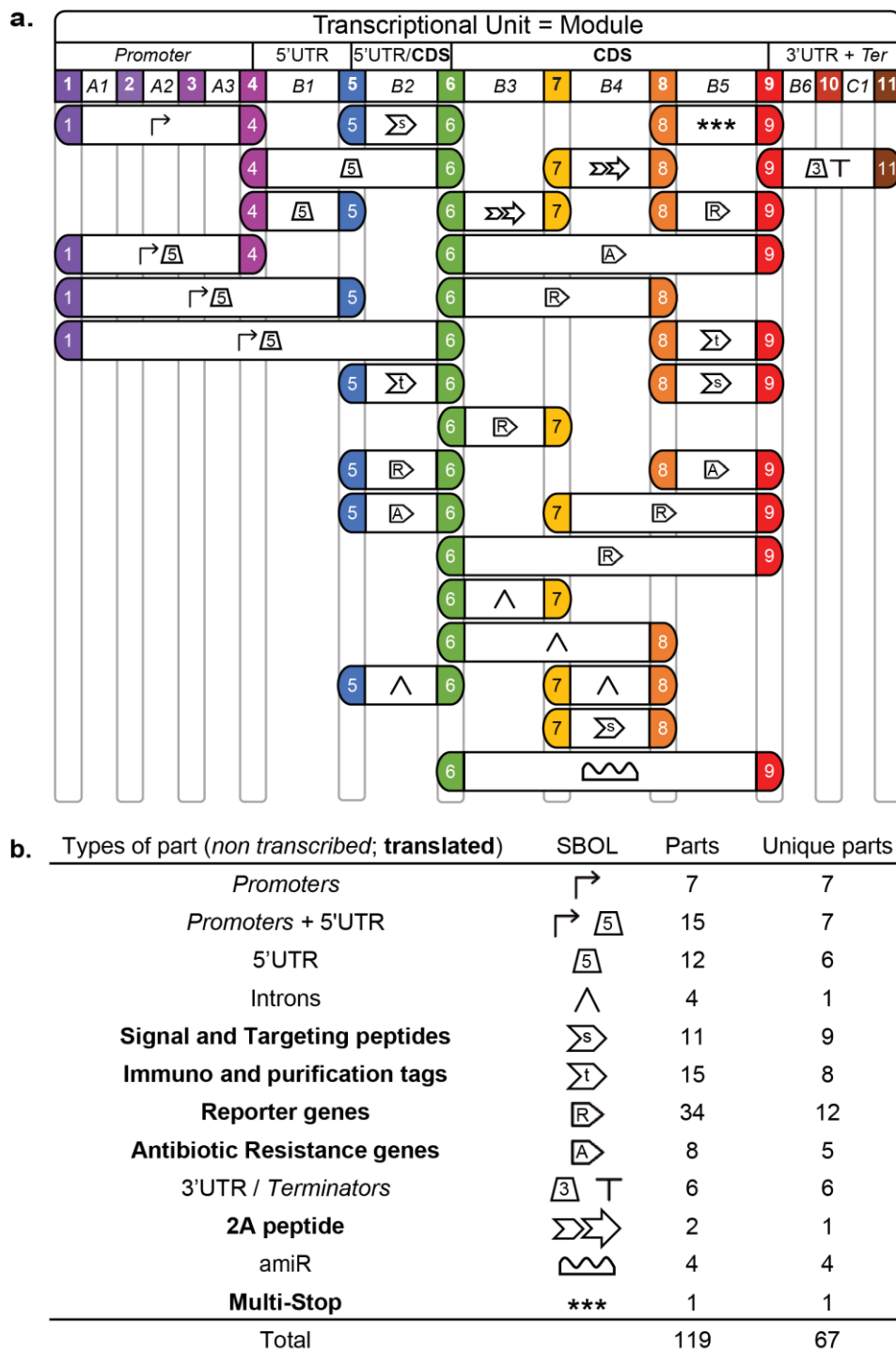
695

696 **Graphical Abstract**



697

Figure 1.



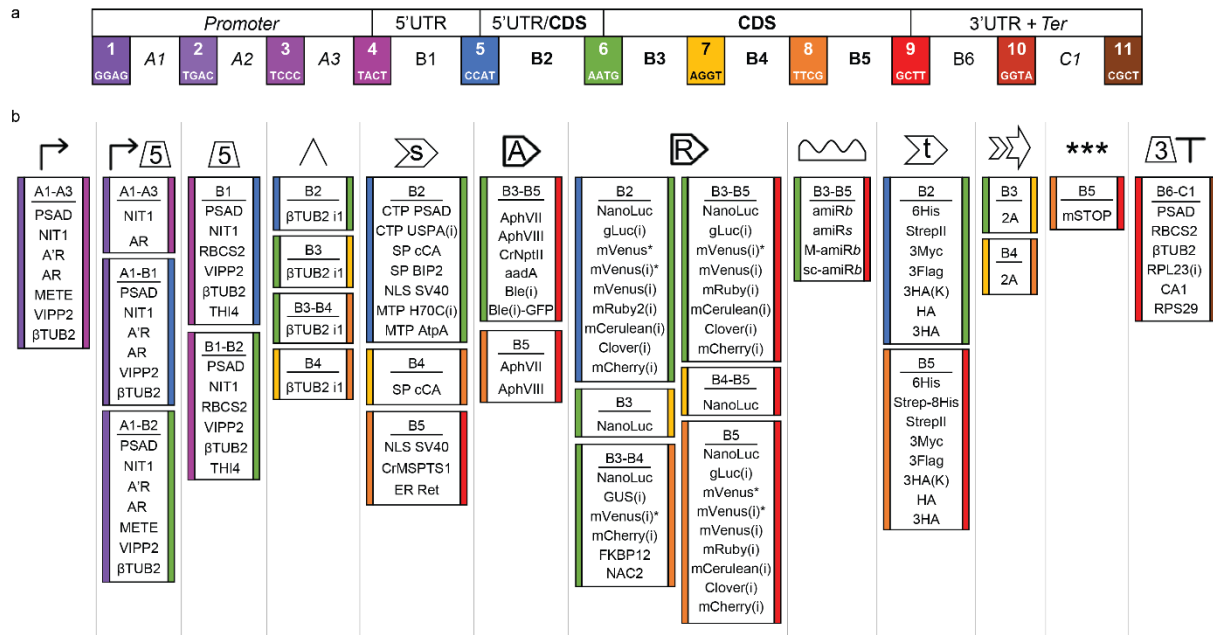
699

700 **Figure 1.** Overview of the Chlamydomonas MoClo toolkit.

701 (a) Type and position of parts used following the Plant MoClo Syntax<sup>30</sup>. Symbols correspond to the SBOL2.0  
 702 visual<sup>69</sup> representation described in **b**. Each of the 11 fusion sites defining a part position is represented with a  
 703 color and a number. Positions presented are representative of the whole set of each part type. Parts in  
 704 italicized letters are non-transcribed, parts in regular letters are transcribed and parts in bold letters are  
 705 transcribed and translated.

706 (b) Table summarizing unique and total gene parts available. The SBOL2.0 symbols are indicated for each type.  
 707 When the SBOL2.0 standard was not existing for a part type, the symbol proposed before<sup>28</sup> was used, or  
 708 defined here.

Figure 2



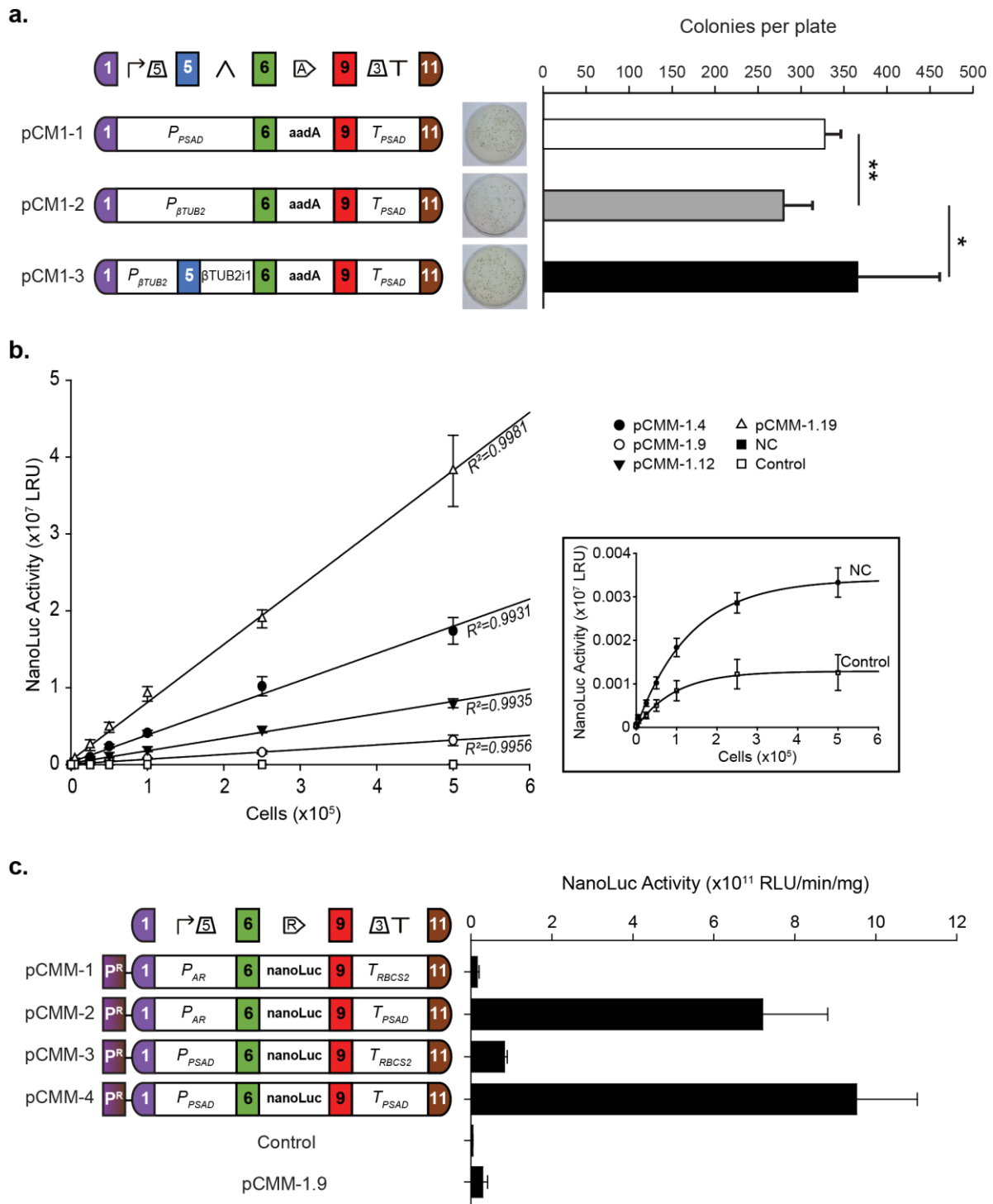
709

710 **Figure 2. List of parts in function of their type and assembly position.**

711 (a) Plant MoClo syntax<sup>30</sup> indicating the color code for fusion sites used in this figure.

712 (b) All parts in the Chlamydomonas MoClo kit are classified primarily by their function, indicated by  
 713 SBOL2.0 visual code<sup>69</sup> as in Fig. 1 (from left to right: promoters, promoter+5'UTR, 5'UTR, introns,  
 714 antibiotic resistance genes, reporter genes, artificial microRNA, immunological and purification tags,  
 715 2A peptide, and 3'UTR+terminators). Colored stripes on the left and right sides of each box represent  
 716 the fusion sites in 5' and 3' of the position, respectively, and follow the color code on top. AR and A'R  
 717 stand for HSP70A/RBCS2 and HSP70A467/RBCS2, respectively<sup>36</sup>. A star (\*) indicates that the part  
 718 contains extra restriction sites as in pOpt vectors<sup>68</sup> while the same part unmarked does not. An (i)  
 719 indicates the presence of an intron within the part (cf. Supplementary Table 2). For amiRNA (amiR)  
 720 backbones, *b* and *s* mean that *Bpi*I and *Spe*I site are within the backbone for amiR cloning,  
 721 respectively, while *M* and *sc* mean that the target amiR sequence for *MAA7* and the control  
 722 scrambled sequence were introduced into the miR1157 backbone, respectively (cf. Fig. 4). mSTOP  
 723 stands for multi-STOP.

Figure 3.



724

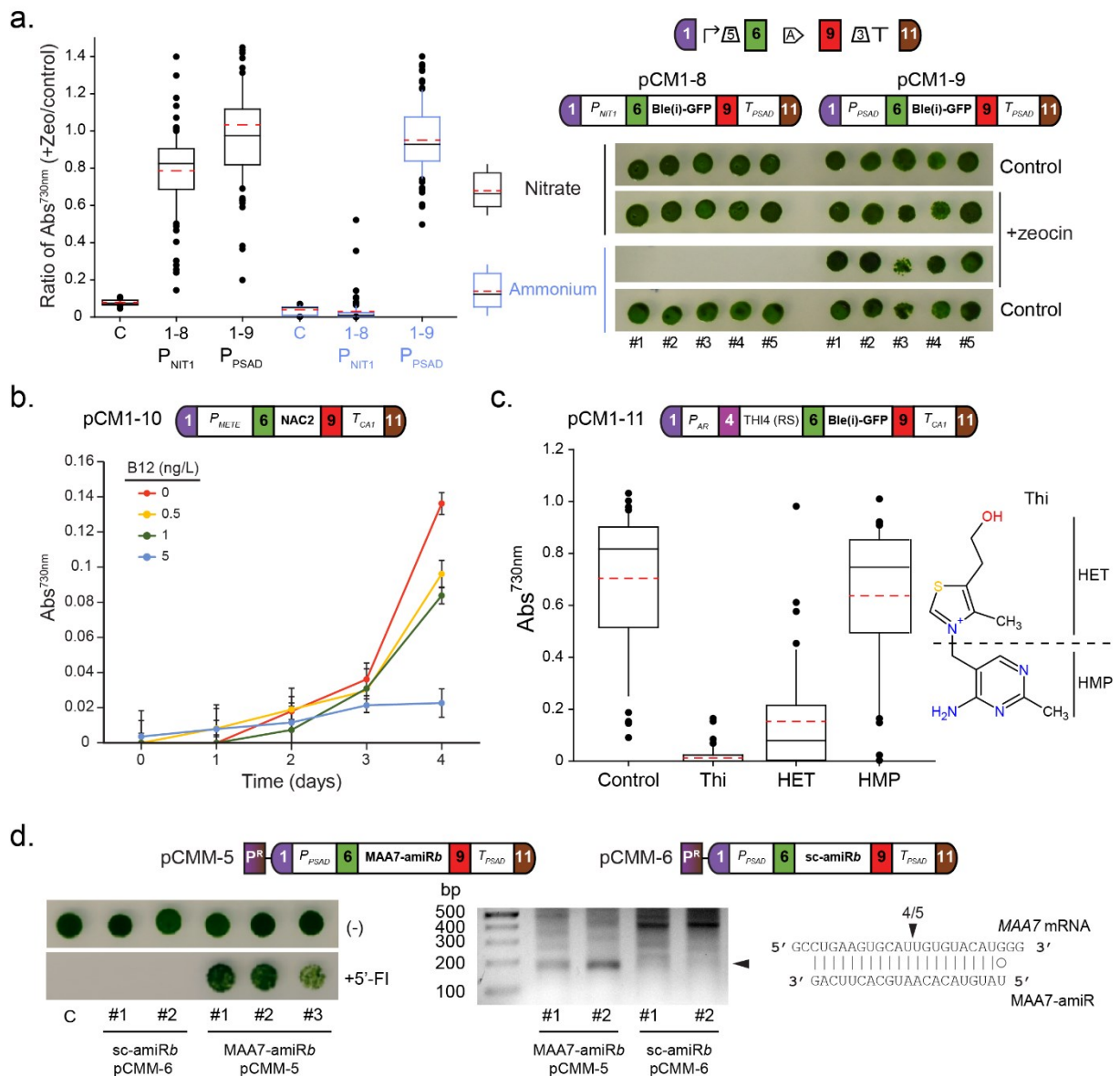
725 **Figure 3.** Constitutive promoters and reporter genes.

726 (a) Average number of spectinomycin resistant colonies after transformation of UVM4 cells (mean  $\pm$   
 727 SD, N=11) for the three modules (pCM1-3, where pCM stands for plasmid Chlamydomonas Moclo).  
 728 Representative transformation plates are shown.

729 (b) Linearity of NanoLuc activity as a function of cell number. NanoLuc activity for 4 independent  
 730 clones transformed with the pCMM-1 device (pCMM-1.X), one non-expressing clone (NC) and the  
 731 recipient strain (CC-4425 noted as control) are presented (N=3, mean  $\pm$  SEM). Linear regression and  
 732 correlation coefficient ( $R^2$ ) are shown. The NC and control are shown in the inset on a different scale.

733 (c) Average NanoLuc activity of D66 (CC-4425) cells transformed with 4 devices (pCMM-1 to 4)  
734 harboring promoter/terminator combinations to drive NanoLuc expression coupled to a  
735 paromomycin resistance module (represented as P<sup>R</sup>, left, Supplementary Fig. 2). Luminescence levels  
736 are represented as mean ± SEM (average of a total of more than 400 clones from 3 biological  
737 replicates). The negative and positive controls are the recipient strain and the pCMM-1.9 strain  
738 (shown in **b**), respectively.  
739 **a,c** \*p<0.05; \*\*p< 0.01 assessed by Student's t-test, SBOL2.0<sup>69</sup> visual of module designs are shown  
740 above the devices.

**Figure 4.**



741

742 **Figure 4. Control of gene expression.**

743 (a) Control of gene expression by the nitrogen source. Zeocin resistant colonies (conferred by *Ble(i)-GFP*)  
 744 selected after transformation of CC-1690 cells with each of the two represented modules (“1-8” for pCM1-8  
 745 and “1-9” for pCM1-9) were grown in TAP-nitrogen ± zeocin (15 µg/mL) supplemented with either 7.5 mM  
 746 (NH<sub>4</sub>)Cl (ammonium, blue) or 4 mM KNO<sub>3</sub> (nitrate, black) and their growth was followed (Absorbance at 730  
 747 nm). The plot shows the ratio between the growth in the presence and absence of zeocin (C is the non-  
 748 transformed CC-1690 strain). The right panel shows cells grown in similar conditions but on solid media. Results  
 749 presented (N=16 for control CC-1690 and N=86 for each other conditions) correspond to one out of three  
 750 independent transformations (for the other two, see Supplementary Fig. 3).

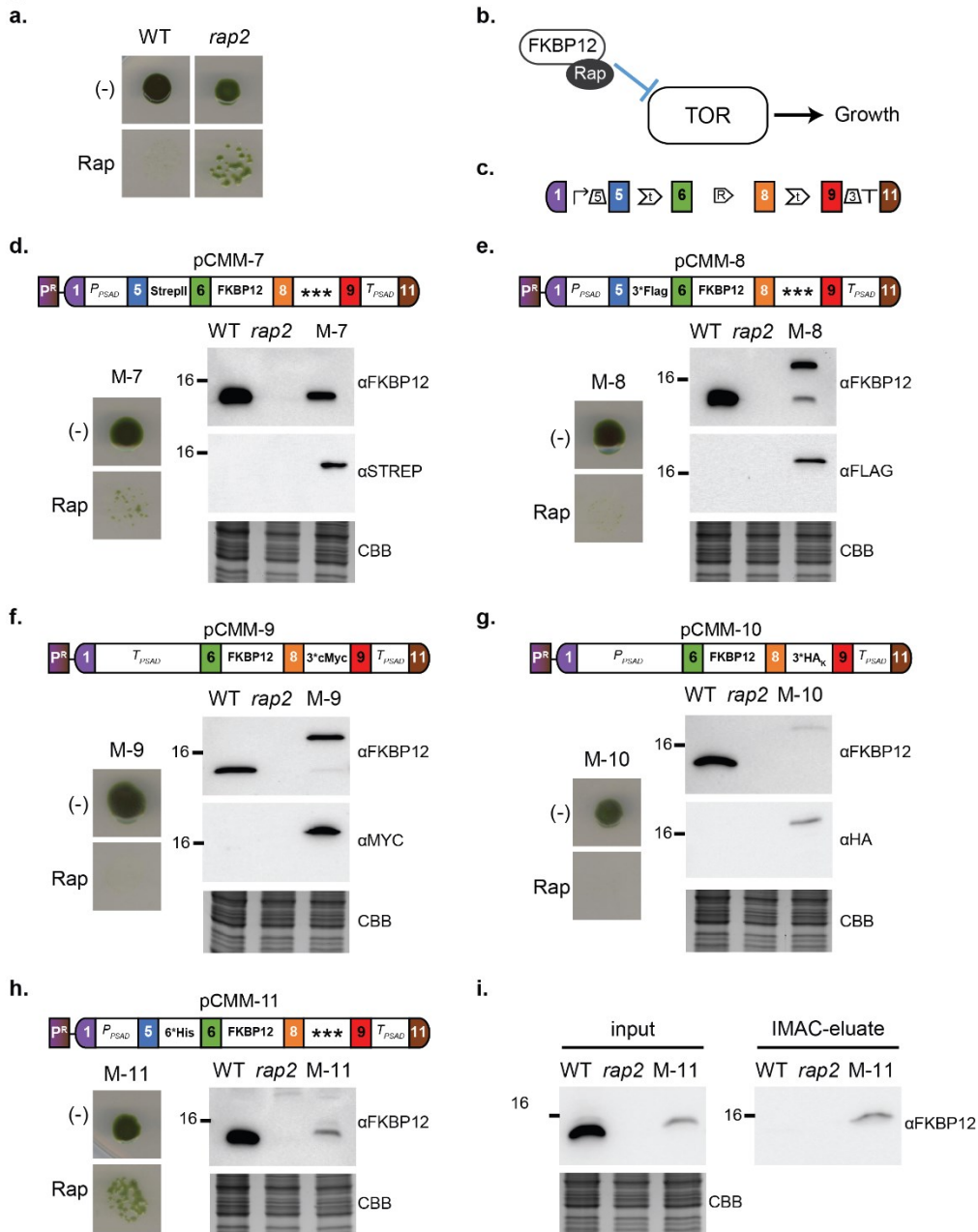
751 (b) Control of gene expression by vitamin B<sub>12</sub>. Conditional complementation of *nac2-26* cells with the pCM1-10  
 752 module expressing NAC2 under *P<sub>METE</sub>* control. Complemented strains were selected for photoautotrophic  
 753 growth on solid minimal medium and the cells were grown in liquid minimal medium supplemented with the  
 754 indicated amount of vitamin B<sub>12</sub>. Data are mean ± SD (N=3).

755 (c) Control of gene expression by vitamin B<sub>1</sub>. Average growth (absorbance at 730 nm after 7 days of growth,  
 756 N=40) of UVM4 cells transformed with the pCM1-11 module designed to express constitutively *Ble(i)-GFP*  
 757 transcripts containing the *THI4* riboswitch in the 5’UTR. After culture in TAP, the cells were transferred to  
 758 TAP+zeocin (10 µg/mL) supplemented with 10 µM thiamine (Thi), 10 µM 4-methyl-5-(2-hydroxyethyl) thiazole

759 (HET) or 10  $\mu$ M 4-amino-5-hydroxymethyl-2-methylpyrimidine (HMP) or not (control). The chemical structure  
760 of Thi is represented on the right and the HET and HMP moieties are indicated (See also Supplementary Fig. 3).  
761 **(d)** Targeted gene knockdown with artificial miRNA. Paromomycin resistant cells selected after transformation  
762 of CC-1690 cells by each of the two represented devices (pCMM-5 and pCMM-6), carrying an amiRNA cloned  
763 with *Bpil* and directed against *MAA7* (*MAA7-amiRb*) or a random sequence ('scrambled': *sc-amiRb*), were  
764 grown in the absence (denoted (-)) or presence of 5'-fluoroindole (+5'-FI) (left panel). C indicates non-  
765 transformed cells. Clones resistant to 5'FI were analyzed by a modified 5'-RACE assay. A specific 173 bp PCR  
766 band (black arrowhead) was amplified only from the 5'-FI resistant transformants and not from ones expressing  
767 the amiRNA with scrambled sequence (middle panel and Supplementary Fig. 3). Sequencing revealed that the  
768 most frequent cleavage occurred at positions opposed to positions 10 and 11 of the amiRNA (right panel, black  
769 arrowhead). P<sup>R</sup> represents the paromomycin resistance module (pCM1-27, Supplementary Fig. 2a).  
770 **a, c** The box and whisker plots show the 10<sup>th</sup> (lower whisker), 25<sup>th</sup> (base of box), 75<sup>th</sup> (top of box) and 90<sup>th</sup> (top  
771 whisker) percentiles. The line within the box is the median, the dashed red line is the mean. Outliers are  
772 plotted as individual data points.  
773



**Figure 5.**



774

775

**Figure 5. Design, build and test of five fusion tags**

776 (a) Phenotype of recipient (WT) and  $\Delta$ *FKBP12* (*rap2*) strains in the presence (Rap) or absence (-) of 1  $\mu$ M  
 777 rapamycin.

778 (b) Molecular mechanism underlying the *rap2* phenotype. Target Of Rapamycin (TOR) is inhibited by rapamycin  
 779 only in the presence of FKBP12 (mutated in *rap2*). Upon formation of the tripartite TOR/FKBP12/rapamycin  
 780 complex, TOR is inhibited and growth is arrested<sup>52</sup>.

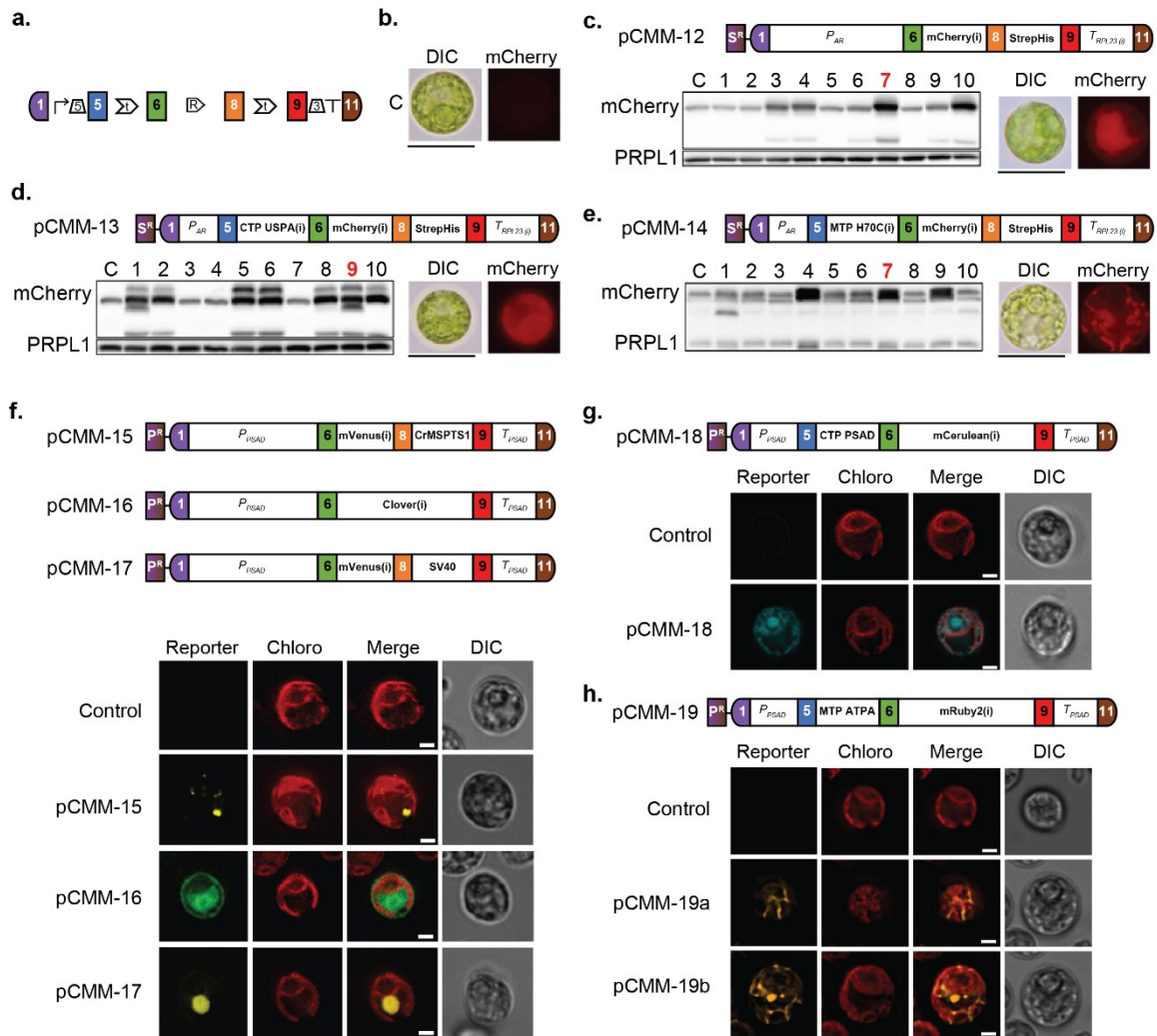
781 (c) SBOL2.0 visual<sup>69</sup> of module designs for functional complementation of *rap2*.

782 (d-h) Phenotype in the presence (Rap) or absence (-) of 1  $\mu$ M rapamycin and detection of tagged proteins in  
 783 soluble extracts by immunoblotting with antibodies against either FKBP12 ( $\alpha$ FKBP12) or the appropriate tag  
 784 (indicated within each panel). Each device is indicated in the upper part of the panel. CBB: Coomassie Brilliant  
 785 Blue staining of a duplicate gel loaded with the same samples and shown as loading control.

786 (i) Purification through ion-metal affinity chromatography (IMAC) of 6His-FKBP12 expressed from the same  
 787 device as in h.

788 P<sup>R</sup> represents the paromomycin resistance module (pCM1-27, Supplementary Fig. 2a). *rap2* cells transformed  
 789 with pCMM-X are indicated as M-X in each panel. Data are representative of 3 biological replicates.

**Figure 6.**



790

791

**Figure 6. Targeting reporter genes to different subcellular compartments.**

792

(a) SBOL2.0<sup>69</sup> visual syntax for modules used.

793

(b) Visible light (“DIC”) and fluorescence signal (“mCherry”) of the UVM4 recipient strain used as control (“C”) for panels c-e.

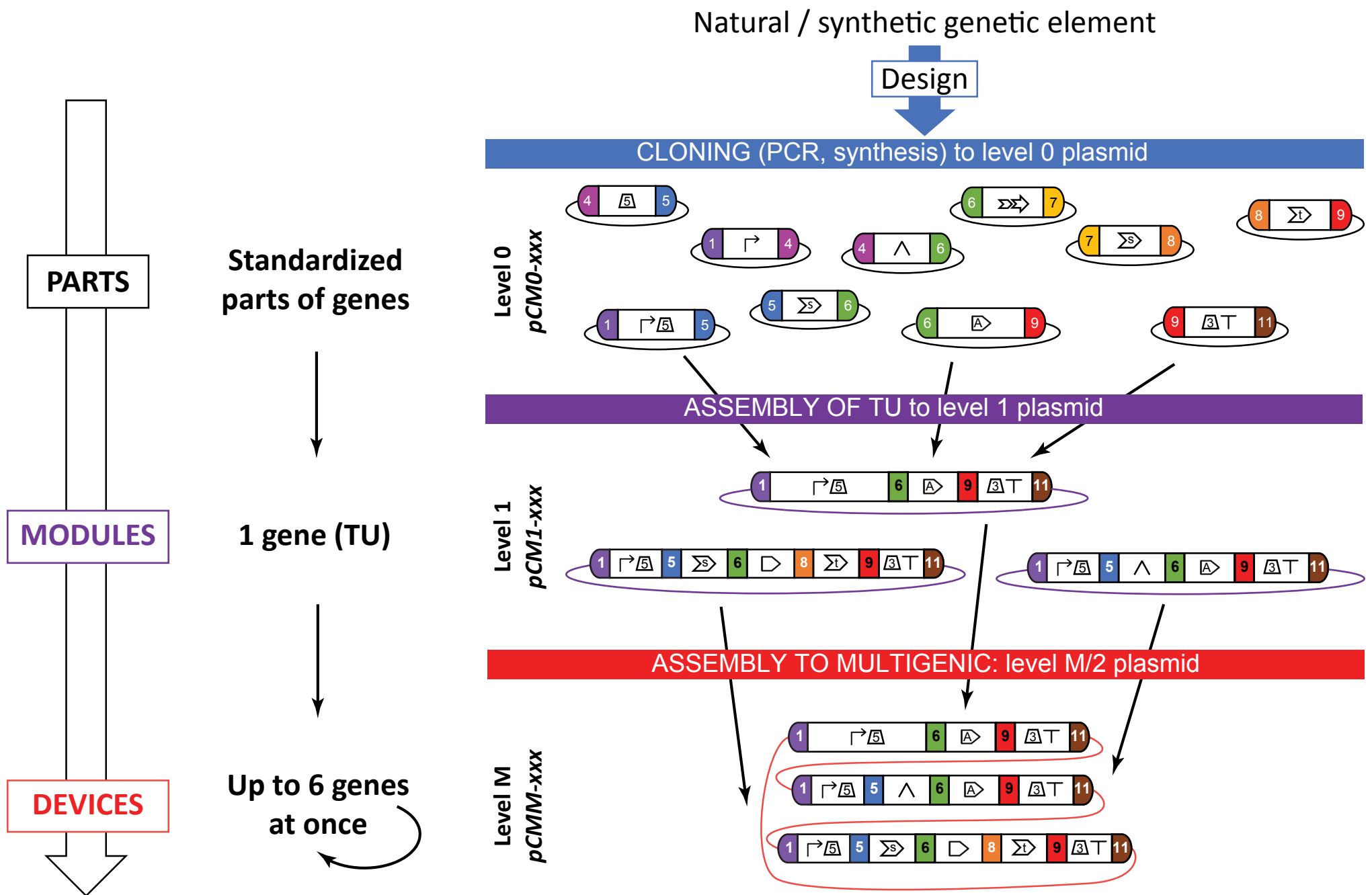
794

(c-e) mCherry targeting to the (c) cytosol with no transit peptide, (d) chloroplast with CTP USPA (Chloroplast Transit Peptide of Universal Stress Protein A) or (e) mitochondria with MTP H70C (Mitochondrial Transit Peptide of HSP70C) in UVM4 cells transformed with the indicated devices (pCMM-12 to 14). In each panel, an anti-mCherry immunoblot analysis of transformants is shown. Note that the anti-mCherry antibody cross-reacts with a protein of similar size present in control cells (C). An anti-PRPL1 immunoblot is shown as loading control. The transformant strain number indicated in red corresponds to the images (bars are 10 μm) presented on the right.

801

(f-h) Fluorescent marking of (f) microbodies with mVenus-CrMSPTS1 (Malate Synthase PTS1-like sequence), cytosol with Clover or the nucleus with mVenus-SV40 (Simian Virus 40 nuclear localization signal), (g) the chloroplast with CTP PSAD-mCerulean (Chloroplast Transit Peptide of PSAD), (h) mitochondria with MTP ATPA-mRuby2 (Mitochondrial Transit Peptide of ATPA) after transformation of UVM4 cells with the indicated devices (pCMM-15 to 19). Images of representative transformants are grouped with the corresponding control image (recipient strain) according to the filter used. pCMM-19a and pCMM-19b show two images taken on different z-axis on the same cell. “Chloro” refers to chlorophyll autofluorescence. The Scale bars represent 2 μm. S<sup>R</sup> and P<sup>R</sup> represent respectively modules conferring resistance to spectinomycin (S<sup>R</sup>=pCM1-1, Fig. 3a and Supplementary Fig. 2a) and paromomycin (P<sup>R</sup>=pCM1-27, Supplementary Fig. 2a).

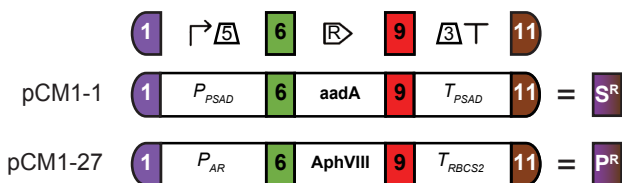
810



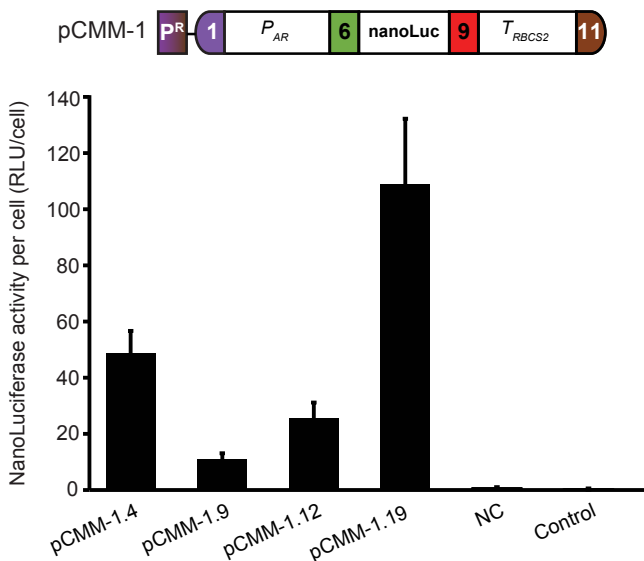
**Supplementary Figure 1. MoClo assembly workflow reflecting the abstraction hierarchy.**

We followed the original MoClo syntax<sup>22</sup> updated<sup>30</sup>. After design of a gene part controlled in silico for full compatibility until level M assembly, the part is cloned with *Bpil* (equivalent to *BbsI*) into the appropriate level 0 plasmid (Spectinomycin bacterial resistance). After quality control (QC) by restriction and sequencing, the resulting clone is registered in the part database as a pCM0-xxx (where pCM stands for plasmid Chlamydomonas Moclo). To generate the desired Transcriptional Unit (TU), the compatible parts are assembled with *BsaI* into the appropriate level 1 plasmid (Ampicillin bacterial resistance). After QC by restriction, the clone is registered as pCM1-xxx in the module database. Finally, to assemble a device, up to 6 modules at a time are assembled with the corresponding end-linker<sup>22</sup> by *Bpil* into a level M or 2 plasmid (Spectinomycin or kanamycin bacterial resistance, respectively). After QC by restriction, the clone is registered as pCMM-xxx in the device database. New assembly from this device can be performed to assemble more modules to the device<sup>22</sup>. Parts are represented in SBOL2.0 visual code<sup>69</sup> (see also Fig. 1).

a.



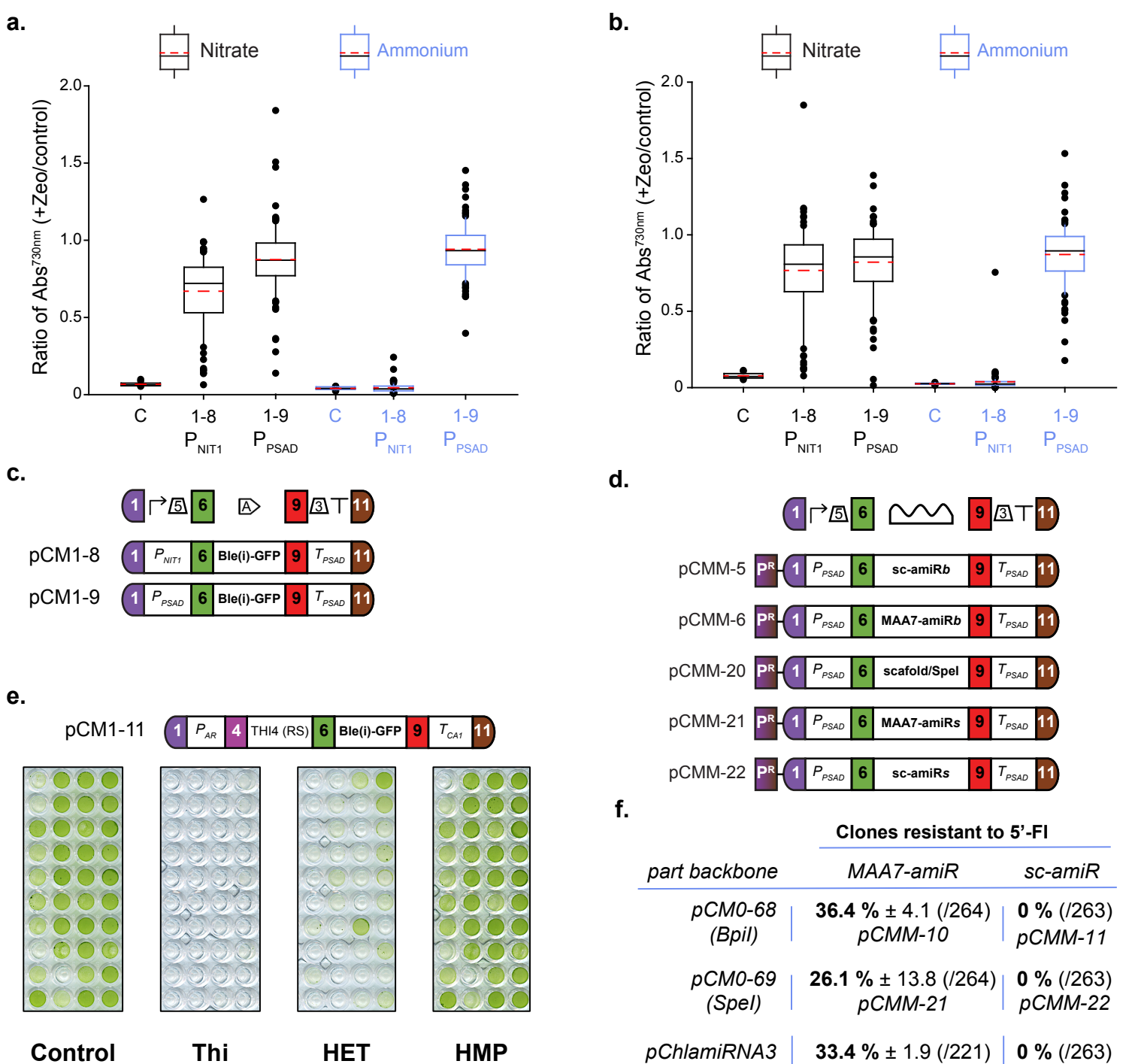
b.



### Supplementary Figure 2. Variability of NanoLuc expression in pCMM-1 transformants.

a. Schemes of the spectinomycin ( $S^R$ ) and paromomycin ( $P^R$ ) resistance modules.

b. NanoLuc activity averaged ( $N=3$ , mean  $\pm$  SEM) per line and expressed as RLU (Relative Luminescence Unit) per cell (same data as in Fig. 3b) of four independent NanoLuc-expressing transformants, one non-expressing clone (noted NC) and the recipient strain (CC-4425, noted control).



### Supplementary Figure 3. Control of gene expression, complementary data.

**(a-b)** Results from the two additional transformation assays performed independently from that presented in Fig. 4a. Control of gene expression by the nitrogen source. Zeocin resistant colonies (*Ble*) selected after transformation of CC-1690 cells by each of the two represented modules (“1-8” stands for pCM1-8 and “1-9” for pCM1-9,) were grown in TAP-nitrogen ± zeocin supplemented with either 7.5 mM (NH<sub>4</sub>)Cl (ammonium, blue) or 4 mM KNO<sub>3</sub> (nitrate, black) and their growth was followed (absorbance at 730 nm). The plot shows the ratio between growth in the presence and absence of zeocin (C is non-transformed CC-1690). Results presented (N = 16 for CC-1690 “C” and N=86 for all others) correspond to two out of three independent transformations (the other is shown in Fig. 4a). The box and whisker plots show the 10th (lower whisker), 25th (base of box), 75th (top of box) and 90th (top whisker) percentiles. The line within the box is the median, the dashed red line is the mean. Outliers are plotted as individual data points.

**(c)** Modules used to generate data presented in figure 4a and in **a** and **b**.

**(d)** Modules used to generate results presented in figure 4d and in **f**.

**(e)** Module used to generate results presented in Figure 4c (top) and image of the cultures used to generate these data. Cultures in TAP+zeocin supplemented or not (control) with 10 μM of thiamine (Thi), 10 μM of 4-methyl-5-(2-hydroxyethyl) thiazole (HET), or 10 μM of 4-amino-5-hydroxymethyl-2-methylpyrimidine (HMP).

**(f)** Percentage of transformants resistant (± SD) to the metabolic drug 5-fluoroindole (5'-FI, used at 20 μM). The CC-1690 strain was transformed with devices (indicated under each result, design in d) containing the amiRNA sequence targeting the *MAA7* gene or a scrambled sequence as a negative control, cloned into the amiRNA backbone with *Bpil* or *SpeI*, corresponding to parts pCM0-79 and pCM0-80, respectively. The pChlamiRNA3 construct containing the same miRNA backbone was used as a positive control. Average of three independent transformations, the total number of transformants screened for 5'-FI resistance in each experiment is indicated in parenthesis.